AD_____

Award Number: W81XWH-06-1-0148

TITLE: Enhancing Tumor Drug Delivery by Laser-Activated Vascular Barrier Disruption

PRINCIPAL INVESTIGATOR: Bin Chen, Ph.D.

CONTRACTING ORGANIZATION: University of the Sciences in Philadelphia
Philadelphia, PA 19104

REPORT DATE: December 2008

TYPE OF REPORT: Annual

PREPARED FOR: U.S. Army Medical Research and Materiel Command
Fort Detrick, Maryland 21702-5012

REPORT DOCUMENTATION PAGE

Form Approved
OMB No. 0704-0188

1. REPORT DATE	2. REPORT TYPE	3. DATES COVERED
1 Dec 2008	Annual	30 Nov 2007 – 29 Nov 2008

4. TITLE AND SUBTITLE

Enhancing Tumor Drug Delivery by Laser-Activated Vascular Barrier Disruption

5a. CONTRACT NUMBER

5b. GRANT NUMBER
W81XWH-06-1-0148

5c. PROGRAM ELEMENT NUMBER

6. AUTHOR(S)

Bin Chen, Ph.D.
Chong He, Ph.D.

E-Mail: b.chen@usp.edu

5d. PROJECT NUMBER

5e. TASK NUMBER

5f. WORK UNIT NUMBER

7. PERFORMING ORGANIZATION NAME(S) AND ADDRESS(ES)

University of the Sciences in Philadelphia
Philadelphia, PA 19104

8. PERFORMING ORGANIZATION REPORT NUMBER

9. SPONSORING / MONITORING AGENCY NAME(S) AND ADDRESS(ES)
U.S. Army Medical Research and Materiel Command
Fort Detrick, Maryland 21702-5012

10. SPONSOR/MONITOR'S ACRONYM(S)

11. SPONSOR/MONITOR'S REPORT NUMBER(S)

12. DISTRIBUTION / AVAILABILITY STATEMENT
Approved for Public Release; Distribution Unlimited

13. SUPPLEMENTARY NOTES

14. ABSTRACT
An obstacle to successful cancer drug therapy is the existence of drug delivery barriers, which causes insufficient drug delivery to the tumor tissue. Because of the inadequate drug delivery, the drug dose has to be increased, which leads to normal tissue toxicity. This delivery problem not only limits the clinical application of existing chemotherapeutics, but also decreases the effectiveness of many new drugs under development for prostate cancer. We found that vascular targeting photodynamic therapy (PDT), a modality involving the combination of a photosensitizer and laser light, is able to disrupt tumor vascular barrier, a significant hindrance to drug delivery. Therefore, tumor accumulation of circulating molecules is significantly enhanced, which has been demonstrated by intravital fluorescence microscopy and whole-body fluorescence imaging techniques. Immunofluorescence staining of endothelial cytoskeleton structure further indicates microtubule depolymerization, stress actin fiber formation and intercellular gap formation. Based on these results, we are using this laser-based therapy to enhance anticancer drug effectiveness. PDT is currently in worldwide multicenter clinical trials for the localized prostate cancer therapy. The available results indicate that PDT employing advanced laser fiber technology and sophisticated light dosimetry is able to treat localized prostate cancer in an effective and safe way. The combination of photosensitization with current chemotherapy or other new drug therapies will further improve its treatment for the localized prostate cancer patients that accounts for more than 90% of total prostate cancer population.

15. SUBJECT TERMS
Photodynamic therapy, verteporfin, tumor vascular targeting, vascular permeability, imaging

16. SECURITY CLASSIFICATION OF:			17. LIMITATION OF ABSTRACT	18. NUMBER OF PAGES	19a. NAME OF RESPONSIBLE PERSON
a. REPORT	b. ABSTRACT	c. THIS PAGE			USAMRMC
U	U	U	UU	37	19b. TELEPHONE NUMBER *(include area code)*

Table of Contents

Introduction

An obstacle to successful cancer drug therapy is the existence of drug delivery barriers, which results in insufficient and heterogeneous drug delivery to the tumor tissue. This drug delivery problem not only limits the clinical application of existing chemotherapeutics, but also decreases the effectiveness of many new drugs under development. Photodynamic therapy (PDT), a modality involving the combination of a photosensitizer and laser light, is an established cancer therapy. Over the past years, we have been focusing on studying PDT as a modality for tumor vascular targeting. Our results demonstrate that vascular-targeting PDT can be used to eradicate tumor tissue, and modify vascular barrier function for an enhanced drug delivery as well. This project will study in detail how vascular photosensitization permeabilizes blood vessels and the influence of photodynamic vascular targeting on tumor vascular function and drug delivery. We rely on various imaging modalities to address these questions. The imaging modalities used in this project include both dynamic live animal/cell imaging that is capable of providing longitudinal information in real time and static ex vivo imaging that is able to reveal biological details at high resolution.

Body

Task 1. To investigate the molecular mechanisms by which photosensitization disrupts endothelial barrier function (months 1-12).

(a). Assess the correlation between photosensitization-induced microtubule disassembly and increase in endothelial cell permeability. The purpose of this study is to determine the role of microtubules in photosensitization-induced endothelial barrier function alteration (months 1-4).

We have found that microtubules play an important role in photosensitization-induced endothelial morphological and functional changes. These results have been published in *Clin Cancer Res.* 2006, 10: 917-23.

(b). Elucidate the mechanism by which photosensitization-induced microtubule depolymerization triggers endothelial cell morphological and functional changes.

We have investigated the mechanism involved in PDT-induced endothelial cell morphological and functional changes. Our results indicate that multiple factors can contribute to endothelial cell function disruption. We have found that verteporfin-PDT induced the formation of reactive oxygen species and the release of calcium. Calcium release has been shown to cause the microtubule depolymerization and induce endothelial cell morphological changes. We also found that PDT induced dephosphorylation of myosin light chain kinase (MLCK), but caused phosphorylation of myosin light chain (MLC). MLC phosphorylation is responsible for endothelial cell contraction. Our results indicate that MLC phosphorylation is independent of MLCK phosphorylation, suggesting that other stimuli are involved in MLC phosphorylation. Currently, we are summarizing our data and a manuscript will be written based on these studies.

Task 2. To determine the functional change and the structural basis of photosensitization-induced vascular barrier compromise (months 1-24)

(a). Intravital microscopic study of photosensitization-induced vascular functional changes.

We have used intravital fluorescence microscopy to continuously monitor tumor blood flow velocity, vessel diameter and vascular permeability in the orthotopic MatLyLu rat prostate tumors after vascular-targeting PDT using three different doses of photosensitizer verteporfin (0.25, 0.5 and 1.0 mg/kg). These results have been published in a recent issue of *Pharmaceutical Research* (see paper reprint in the appendix). We found that effects of PDT on blood perfusion and vascular permeability followed a reverse dose dependence. A higher dose of verteporfin PDT was more effective in inducing perfusion disruption, but less effective in enhancing vascular permeability and macromolecule accumulation. These results indicate that a lower dose of verteporfin PDT is more favorable for enhancing tumor drug delivery.

(b). Assessment of tumor uptake of fluorescence probes with different sizes.

We have used intravital fluorescence microscopy to compare the tumor accumulation of fluorochrome-labeled dextran molecules with molecular weight of 155 and 2000 kDa after three different doses of photosensitizer verteporfin (0.25, 0.5 and 1.0 mg/kg). We found that PDT using verteporfin was more effective in enhancing the tumor accumulation of a lower molecular weight dextran molecule than a higher molecular weight dextran molecule (*Pharm Res*. 2008, 25: 1873-1880 in the appendix).

Since most chemotherapeutic agents tend to be associated with albumin in circulation, we use a whole body fluorescence imaging system to monitor TRITC-albumin tumor uptake in real time on live animals. We found that vascular leakage of fluorescence-labeled albumin (TRITC-albumin) was significantly increased after the vascular-targeting PDT, as compared to the control tumor. Interestingly, PDT-induced increase in TRITC-albumin accumulation was especially pronounced in the tumor periphery. To further confirm these macroscopic imaging results, we sacrificed animals at various time points and excised tumor tissues for fluorescence microscopic study. Similar to the whole body tumor images, TRITC-albumin was found to have more accumulation in the tumor periphery. These results have recently been published in the *International Journal of Cancer* (see paper reprint in the appendix).

(c). Determine blood vessel structural changes induced by photosensitized vascular permeabilization.

We have performed light and electron microscopy to examine vessel structural changes after PDT. At the light microscopy level, we have found that PDT induced vessel dilation and occlusion at early time points after treatment, which progress to severe vessel degeneration and rapture at late times (*Int J Cancer*. 2008, 123: 695-701). At the electron microscopy level, we found platelet aggregation, thrombus formation and endothelial cell rupture (**Fig 1**). All these findings demonstrate that PDT damages endothelial cells, which induce platelet aggregation and vascular shutdown.

We also performed immunohistochemistry to stain vessel endothelial marker CD31, pericyte marker smooth muscle actin and basement membrane marker Type IV collagen. We found that PDT caused a loss of CD31 staining, again suggesting direct endothelial damage. Interestingly, we found that tumor tissues showed spatial variation in the vessel supporting structure. Central blood vessels generally don't have open lumen and have less coverage of vessel supporting structure (see book chapter in the appendix). This might explain the disparity between interior and peripheral vasculature in vascular response to vascular-targeting PDT.

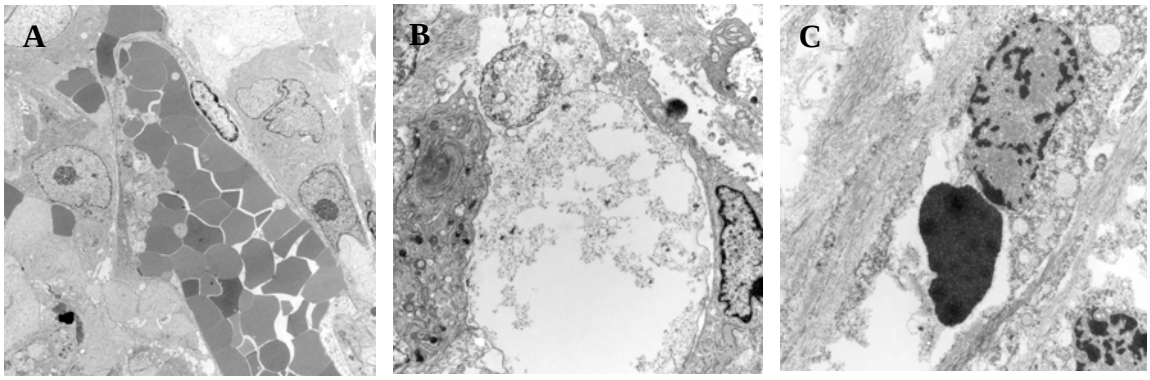

Fig. 1. The electron microscopic photographs showing vascular damage after vascular-targeting PDT. The PC3 human prostate tumors were treated with vascular-targeting PDT (40 J/cm^2 at 15 min after 0.5 mg/kg verteporfin (i.v.)). (A) 1 h after PDT showing platelet aggregation and thrombus formation; (B) 6 h after PDT showing edema, endothelial cell degeneration and vessel rupture; (C) 24 h after PDT showing endothelial cell death, vessel rupture and tumor cell death.

Task 3. To explore the potential of improving tumor drug delivery and therapeutic effect by photosensitized vascular permeabilization (months 25-36).

a. Fluorescence imaging, microscopy & flow cytometry analysis of tumor drug distribution and penetration.

Bevacizumab, a FDA-approved recombinant humanized monoclonal antibody (MW 149 kDa) against VEGF, was used in this study. To visualize the distribution of bevacizumab, we have labeled bevacizumab with Alex Fluor 647 dye using Invitrogen small animal in vivo imaging protein labeling reagents. We found that vascular targeting PDT using verteporfin was able to preferentially enhance the accumulation of bevacizumab at the tumor periphery where tumor recurrence tended to occur. We also found that PDT induced VEGF overexpression at peripheral tumor area. The overexpression of VEGF at tumor periphery might be responsible for peripheral tumor recurrence. Based on these results, we continue to examine the effects of PDT in combination with bevacizumab on tumor regrowth.

b. Evaluate tumor response following the combination of anticancer agent and verteporfin-photosensitization.

We have evaluated tumor response following the combination of vascular targeting PDT and bevacizumab in the PC-3 human prostate tumor model. As shown in **Fig 2**, the average tumor volume in the group of animals treated with the combination therapy is only about half of the PDT alone group. These results indicate that PDT using verteporfin in combination with bevacizumab leads to an enhanced therapeutic effect.

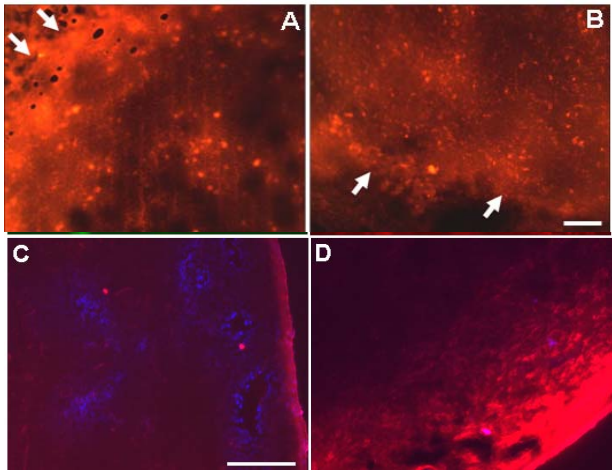

Fig 2. (A, B) PDT with verteporfin induces VEGF overexpression in tumor peripheral areas. The MatLyLu tumor was treated with verteporfin-PVTT (50 J/cm^2 light treatment at 15 min after 0.25 mg/kg dose of verteporfin). Tumor sections taken at 3 h after treatment were stained for VEGF expression. **(A)** verteporfin-PVTT; **(B)** untreated control. Arrows indicate tumor peripheral areas. Bar, 100 um.

(C, D) Effects of PDT on Alexa 647-bevacizumab distribution. PC-3 tumors were treated with verteporfin-PDT (50 J/cm^2 light treatment at 15 min after 0.5 mg/kg dose of verteporfin). Control tumors received no treatment. Animals were i.v. injected with 50 mg/kg Alexa 647-bevacizumab immediately after treatment. Tumor sections were taken at 24 h after treatments. Red fluorescence shows the distribution of bevacizumab and blue fluorescence indicates functional blood vessels visualized by Hoechst dye. **(C)** Control; **(D)** PDT. Bars, 100 um.

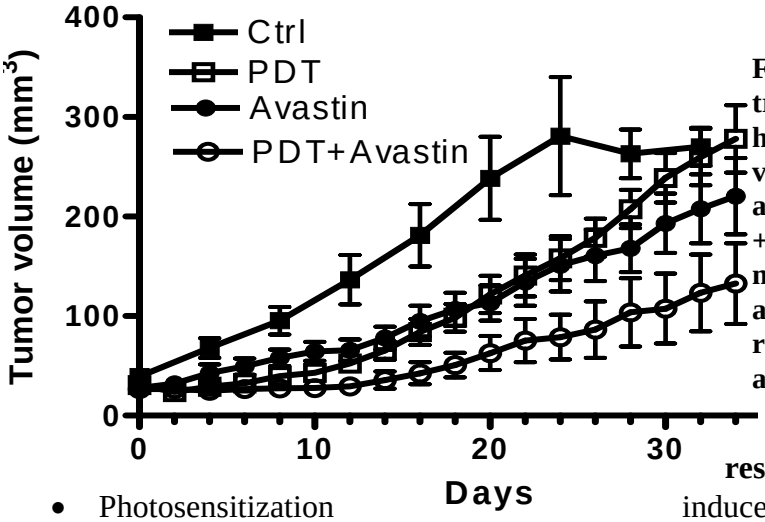

Fig. 5. Tumor regrowth curve after different treatments. For the PDT only group, PC3 human prostate tumors were treated with vascular-targeting PDT (40 J/cm^2 at 15 min after 0.5 mg/kg verteporfin (i.v.)). For the PDT + Ava group, animals were injected with 50 mg/kg Avastin (bevacizumab) immediately after PDT treatment. The control group received no treatment. Each group includes 6-7 animals.

Key research accomplishments

- Photosensitization induces microtubule depolymerization and stress fiber actin formation, leading to endothelial morphological changes and barrier dysfunction.
- Photosensitization induces the formation of reactive oxygen species and calcium release, which induces microtubule depolymerization. Photosensitization causes myosin light chain phosphorylation independent of myosin light chain kinase phosphorylation.
- Vascular-targeting PDT induces time- and dose-dependent decrease in tumor blood flow and increase in vascular permeability.
- PDT-induced vascular barrier dysfunction leads to increased accumulation of circulating molecules in tumor tissues, which can be used to enhance drug delivery to the tumor tissue. Low dose PDT is more effective in enhancing tumor drug delivery than the high dose PDT and PDT-induced drug delivery enhancement is especially pronounced in the tumor periphery.
- PDT is more effective in enhancing the accumulation of macromolecules with a lower molecular weight.
- PDT significantly enhances the distribution of bevacizumab (Avastin) at tumor periphery. Combination of vascular-targeting PDT and antibody drug bevacizumab results in an enhanced anti-tumor effect.

Reportable outcomes

Publications:

Chen B, Pogue BW, Luna J, Hardman R, Hoopes PJ, Hasan T. Tumor vascular permeabilization by vascular-targeting photosensitization: effects, mechanism and therapeutic implications. *Clin Cancer Res.* 2006, 10: 917-23.

Chen B, Pogue BW, Hoopes PJ, Hasan T. Vascular and cellular targeting for photodynamic therapy. *Crit Rev Eukaryot Gene Expr.* 2006, 16: 279-306.

He C, Agharkar P, Chen B. Intravital microscopic analysis of vascular perfusion and macromolecule extravasation after verteporfin-mediated photodynamic therapy. *Pharm Res.* 2008, 25: 1873-80.

Chen B, Crane C, He C, Gondek D, Agharkar P, Savellano M, Hoopes PJ, Pogue BW. Disparity in vascular response to verteporfin-mediated vascular-targeting therapy between prostate tumor interior versus peripheral vasculature. *Int J Cancer.* 2008, 123: 695-701.

Book chapter:

Chen B, He C, de Witte P, Hoopes PJ, Hasan T, Pogue BW. "Chapter 9: Vascular Targeting in Photodynamic Therapy" in *Michael R. Hamblin & Pawel Mroz (Editors), Advances in Photodynamic Therapy: Basic, Translational and Clinical, pp 179-91, Norwood, MA: Artech House Inc. 2008.*

Abstracts:

Agharkar P, Chen, B. Elucidating the mechanisms of photodynamic therapy induced endothelial cell morphological and functional change. *The 34th Meeting of the American Society for Photobiology (June 20-25, 2008, Burlingame, CA), page 6.*

He C, Agharkar P, Chen, B. Intravital microscopic analysis of vascular perfusion and macromolecule extravasation after photodynamic vascular targeting therapy. *The 34th Meeting of the American Society for Photobiology (June 20-25, 2008, Burlingame, CA), page 39.*

Chen B, He C, Crane C, Pogue BW. Fluorescence imaging of verteporfin-mediated photodynamic therapy targeting prostate tumor vasculature. *The Department of Defense (DoD) Innovative Minds in Prostate Cancer Today (IMPACT) meeting, Sep 5-8, 2007, Atlanta, Georgia.*

Chen B, He C, Crane C, Pogue BW. Fluorescence imaging of verteporfin-mediated photodynamic therapy targeting prostate tumor vasculature. *Program & Abstracts of 11th World Congress of the International Photodynamic Association (IPA, March 28-31, 2007, Shanghai, China).*

Chen B, Pogue BW, Hoopes PJ, Hasan T. Enhancing tumor drug delivery by laser-activated vascular barrier disruption. *The 11th NCI Prouts Neck Meeting on Prostate Cancer (Nov 2-5, 2006, Prouts Neck, Maine), page 32.*

Chen B, Pogue BW, Hoopes PJ, Hasan T. Photodynamic tumor vascular targeting enhances cancer chemotherapy. *The 90th Optical Society of America (OSA) Annual Meeting (Oct 8-12, 2006, Rochester, NY) Conference Program, page 160.*

Chen B, Pogue BW, Hoopes PJ, Hasan T. Effects and mechanisms of vascular permeabilization by vascular-targeting photodynamic therapy. *Conference Proceedings of the 33rd Meeting of the American Society for Photobiology (Jul 8-12, 2006, Puerto Rico), page 65.*

Conclusions

We have found that photodynamic tumor vascular targeting induced significant vascular morphological and functional changes. As a result, tumor accumulation of fluorescence molecular probes with different molecular weight is significantly enhanced after photodynamic vascular targeting. The combination of photodynamic tumor vascular targeting and anticancer agent bevacizumab leads to a synergistic therapeutic effect.

Appendices

He C, Agharkar P, Chen B. Intravital microscopic analysis of vascular perfusion and macromolecule extravasation after verteporfin-mediated photodynamic therapy. *Pharm Res.* 2008, 25: 1873-80.

Chen B, Crane C, He C, Gondek D, Agharkar P, Savellano M, Hoopes PJ, Pogue BW. Disparity in vascular response to verteporfin-mediated vascular-targeting therapy between prostate tumor interior versus peripheral vasculature. *Int J Cancer.* 2008, 123: 695-701.

Chen B, He C, de Witte P, Hoopes PJ, Hasan T, Pogue BW. "Chapter 9: Vascular Targeting in Photodynamic Therapy" in *Michael R. Hamblin & Pawel Mroz (Editors), Advances in Photodynamic Therapy: Basic, Translational and Clinical, pp 179-91, Norwood, MA: Artech House Inc. 2008.*

Pharmaceutical Research, Vol. 25, No. 8, August 2008 (© 2008)
DOI: 10.1007/s11095-008-9604-5

Research Paper

Intravital Microscopic Analysis of Vascular Perfusion and Macromolecule Extravasation after Photodynamic Vascular Targeting Therapy

Chong He,[1] Priyanka Agharkar,[1] and Bin Chen[1,2,3]

Received February 25, 2008; accepted April 16, 2008; published online April 30, 2008

Purpose. Photodynamic therapy (PDT), involving the combination of a photosensitizer and light, is being evaluated as a vascular disrupting therapy and drug delivery enhancement modality based on its effects on vascular perfusion and barrier function. Since tumor vasculature is the common route for the delivery of both blood and therapeutic agents, it is important to compare the effects of PDT on blood perfusion and substance transport.
Materials and Methods. Tumor blood cell velocity and the extravasation of high molecular weight dextran molecules were continuously monitored by intravital fluorescence microscopy for up to 60 min after PDT using three doses of verteporfin in the MatLyLu prostate tumor model.
Results. PDT induced tumor perfusion disruption via thrombus formation. PDT using a higher dose of verteporfin was more effective in inhibiting blood perfusion while a lower dose verteporfin-PDT was more potent in enhancing dextran extravasation. The increase in dextran extravasation induced by PDT was dependent upon dextran molecular weight. A lower molecular weight dextran obtained a higher tumor accumulation after PDT than a higher molecular weight dextran.
Conclusions. PDT with verteporfin had different effects on tumor vascular perfusion *versus* the extravasation of macromolecules. Optimal PDT conditions should be adjusted based on the therapeutic application.

KEY WORDS: benzoporphyrin derivative (BPD); blood flow; drug delivery; photodynamic therapy (PDT); photosensitizer; vascular permeability; vascular targeting.

INTRODUCTION

Tumor vasculature represents an important target for cancer therapy due to the dependence of tumor cells on a functional blood supply for cell growth, and blood-borne therapeutic agents to get access to tumor tissues (1). On the one hand, tumor blood vessels can be targeted by antiangiogenic and vascular disrupting agents to inhibit tumor progression (2). On the other hand, tumor vascular function can be modified to enhance the delivery of anticancer agents to tumor tissues because tumor vasculature is one of the major physiological barriers for sufficient delivery of therapeutic agents to tumor tissues, especially for macromolecular agents (3). Thus, strategies aimed at specifically disrupting the endothelial barrier integrity are being developed to improve delivery of therapeutic agents to the tumor tissues (4).

Photodynamic therapy (PDT) is an established cancer treatment modality, which involves the combination of a photosensitizing compound, light with a wavelength matching the absorption of photosensitizer, and oxygen molecules (5). Upon absorption of light, photosensitizer molecules are activated from the ground state to the triplet state, which then react with oxygen and produce highly reactive singlet oxygen. The mechanism of PDT is complicated, involving a combined effect of photocytotoxicity, vascular damage and immune reactions (6). Photodynamic vascular targeting therapy aims to selectively target tumor vasculature for therapeutic purposes. In this case, laser light is usually delivered to tumor tissues shortly after systematic administration of a photosensitizer when the drug is predominately localized within blood vessels (7). Preferential photosensitization of vascular components leads to vessel functional changes. This vascular-targeting modality has been approved for the treatment of age-related macular degeneration and is currently under clinical trial for prostate cancer treatment (7).

It was recently reported that PDT can be used to facilitate the delivery of macromolecular agents to tumor tissues via induced vascular leakage (8). We demonstrated in the MatLyLu rat prostate tumor model that vascular-targeting PDT with photosensitizer verteporfin significantly increases vascular permeability and tumor accumulation of circulating molecules (9). However, the same treatment was also found to cause vascular shutdown by inducing thrombus formation, resulting in extensive tumor necrosis. Because tumor vasculature is the common route for the delivery of both blood and therapeutic agents, it is important to understand how

[1] Department of Pharmaceutical Sciences, Philadelphia College of Pharmacy, University of the Sciences in Philadelphia, 600 South 43rd Street, Philadelphia, Pennsylvania 19104, USA.
[2] Department of Radiation Oncology, University of Pennsylvania, Philadelphia, Pennsylvania 19104, USA.
[3] To whom correspondence should be addressed. (e-mail: b.chen@usp.edu)

differently vascular-targeting PDT affects tumor perfusion and vascular barrier functions. Such knowledge is crucial to apply this modality for tumor targeting and anticancer drug delivery enhancement. By permitting high resolution imaging of vessel structure and function in live animals, intravital microscopy offers a powerful tool to study vascular morphology and function (10). Here we used this system to examine changes of vessel perfusion and barrier function after verteporfin-PDT targeting tumor blood vessels in an orthotopic rat prostate tumor model.

MATERIALS AND METHODS

Orthotopic Prostate Tumor Model. The orthotopic R3327-MatLyLu Dunning rat prostate tumor model was used in this study. The MatLyLu tumor is an androgen-independent prostate carcinoma, syngeneic to the male Copenhagen rats, and highly metastatic to lymph nodes and lungs (MatLyLu) (11). The MatLyLu cells were maintained in the RPMI-1640 with glutamine (Mediatech, Herndon, VA) supplemented with 10% fetal bovine serum (HyClone, Logan, UT) and 100 units/ml penicillin-streptomycin (Mediatech) at 37°C in a 5% CO_2 incubator. The orthotopic tumors were induced by injecting 1×10^5 tumor cells in the ventral lobe of prostate in the Copenhagen rats (6–8 weeks old, Charles River Laboratories, Wilmington, MA), as described previously (12). Tumors were used for experiments at 7–8 days after implantation with a size of 8–10 mm in diameter. All animal procedures were carried out according to the NIH Principles of Laboratory Animal Care and approved by the Institutional Animal Care and Use Committee (IACUC).

Photosensitizer. Verteporfin (benzoporphyrin derivative (BPD) monoacid ring A in a lipid-formulation) was obtained from QLT Inc. (Vancouver, Canada) as a gift. A stock saline solution of verteporfin was reconstituted according to the manufacturer's instruction and stored at 4°C in the dark. Stock solution of BPD was diluted right before injection.

PDT Treatments. A diode laser system (High Power Devices Inc., North Brunswick, NJ) with 690 nm wavelength was used for the irradiation of MatLyLu tumors. The laser was coupled to an optical fiber with 600 μm core diameter for light delivery. A microlens was connected to the end of fiber to achieve homogeneous irradiation of a 12 mm-diameter spot. The MatLyLu tumors were surgically exposed to illumination with an irradiance of 50 mW/cm^2 for 1,000 s, resulting in a total light dose of 50 J/cm^2. Light intensity was measured with an optical power meter (Thorlabs Inc, North Newton, NJ). Animals were anesthetized with injection (i.p.) of a mixture of ketamine (90 mg/kg) and xylazine (9 mg/kg) during treatment. Three different doses of verteporfin (0.25, 0.5 and 1.0 mg/kg) were examined, which was always i.v. injected at 15 min prior to light irradiation. We have shown in the previous study that verteporfin is primarily localized in the tumor vasculature at this time (13).

Intravital Fluorescence Microscopy. Immediately after PDT treatment, tumor-bearing animals were i.v. injected with 20 mg/kg of Hoechst, 5 mg/kg of fluorescein isothiocyanate-labeled dextran with a molecular weight of 2,000 kilo Dalton (2,000 kDa FITC-dextran), and 10 mg/kg of tetramethylrhodamine isothiocyanate-labeled dextran with a molecular weight of 155 kilo Dalton (155 kDa TRITC-dextran). These three fluorescence dyes (all from Sigma-Aldrich Corp, St. Louis, MO) were bolus injected as a mixture. The anesthetized animals were then placed in a prone position on the microscope stage and the MatLyLu tumors were imaged with a Leica DMI 6000B inverted fluorescence microscope. A microscopic field including clearly visible blood vessels was selected and imaged every 5 min for up to 60 min after injection. A 20× long working distance objective was used to image tumor tissues and different channel fluorescence images were captured with a Hamamatsu ORCA-AG CCD monochrome camera. The multi-channel image acquisition with appropriate filter setup was controlled by SimplePCI software (Compix Inc, Cranberry, PA). All the following image analyses were performed with the SimplePCI and NIH ImageJ software packages.

Analysis of Blood Cell Velocity. Blood cell flow velocity was measured based on the Hoechst channel (excitation: 360/40 nm; emission: 470/40 nm) images, which were captured at a speed of 17 frames per second for 3 s every 5 min after PDT. Hoechst dye stained the nuclei of circulating blood cells. Blood cell flow velocity was calculated by measuring the distance of Hoechst-positive cells traveled between two consecutive images divided by the time interval between these two images. Because the morphological differences between arteriols and venules in tumor tissues are often not distinct, vessels were chosen for velocity measurements solely based on the vessel size. In each animal, blood cell velocity values at different time points after PDT were normalized to the first point value, i.e. 5 min after PDT, to obtain the relative change after treatment. The percentage changes of each animal in the same group were pooled to generate an overall response curve.

Analysis of Blood Vessel Diameter and Fluorochrome-Labeled Dextran Extravasation. The FITC channel (excitation: 480/40 nm; emission: 527/30 nm) and TRITC channel (excitation: 546/12 nm; emission: 600/40 nm) images were captured every 5 min for up to 60 min after PDT with fixed camera settings. Images in each channel were properly oriented and stacked to ensure that measurements were taken at approximately the same location. Blood vessel diameter was measured based on the FITC-dextran images.

To measure the extravasation of fluorochrome-labeled dextrans in tumor tissues, regions of interest (ROIs) with diameter of 10 μm were selected on the FITC channel images. The same ROIs were also marked at same locations on the matched TRITC images. Although close to nearby blood vessels, these ROIs were chosen in areas without visible blood vessels. The average fluorescence intensity in ROIs was measured on the FITC and TRITC images taken at different times after PDT. All intensity values in each ROI were normalized to its first point value, i.e. 5 min after PDT, to obtain percentage changes as a function of time after treatment. Data of ROIs in the same group were pooled to generate the overall response curve. The area under curve (AUC) of each ROI intensity change curve was calculated to

represent the accumulation of fluorochrome-labeled dextran in tumor tissues over the 60 min period.

Statistical Analysis. Blood cell flow velocity, vessel diameter and fluorescence intensity data were first analyzed using repeated measures analysis of variance (ANOVA) with Tukey's post test to examine statistical differences among measurements taken at various time points during the 60 min period after treatment. One-way ANOVA test with Tukey's post test was then used to determine statistical differences between various treatment groups and the control group. Statistical significance was accepted at $p<0.05$. All statistical analyses were carried out using GraphPad Prism software (GraphPad, San Diego, CA).

RESULTS

Thrombus formation and blood flow stasis were two significant observations after PDT treatments. PDT with 0.25 mg/kg dose of verteporfin mainly induced the formation of emboli (unstable thrombi). Although reduction in blood flow was clearly visible, most blood vessels were still functional at the end of 60 min after this PDT treatment possibly due to the dislodging of unstable clots. As shown in Fig. 1, thrombus formation was observed as early as 5 min after 0.5 mg/kg dose of verteporfin-PDT. The development of thrombus caused vessel lumen narrowing and stagnant blood flow, resulting in complete perfusion arrest at 50 min after treatment.

Changes in blood cell flow velocity and vessel diameter were continuously measured for a period of 60 min after treatments and the data were shown in Fig. 2. There was a slight increase in blood cell velocity in control tumors, but this change was not statistically significant ($p>0.05$, Fig. 2A). PDT with 0.25 mg/kg dose of verteporfin induced up to 50% reduction in blood cell velocity after treatment ($p<0.01$). However, among eight blood vessels analyzed, six were still functional at the end of 60 min after PDT. Significant decrease in blood cell velocity was also observed in tumors treated with 0.5 mg/kg dose of verteporfin PDT ($p<0.01$). After a short rebound, blood cell velocity continued to decline to nearly complete perfusion arrest at 60 min after treatment. Only 2 out of 14 vessels analyzed were still functional at the end of observation. PDT with 1.0 mg/kg dose of verteporfin caused complete blood flow arrest within 20 min and no recovery was observed up to 60 min after PDT ($p<0.01$). Similar to control tumors, no significant change in vessel diameter was detected in tumors treated with either 0.25 or 0.5 mg/kg dose of verteporfin PDT ($p>0.05$, Fig. 2B). PDT with 1.0 mg/kg dose of verteporfin induced an initial vessel constriction followed by vessel dilation at late times. However, none of these changes were statistically significant compared to the 5 min time point ($p>0.05$).

Blood vessels analyzed in this study ranged from 0 to 1817.6 μm/s in blood cell velocity and from 8.3 to 83.1 μm in vessel diameter. There was no correlation between blood cell velocity and vessel diameter in control and all three PDT groups at any time point ($p>0.05$). As PDT with 0.5 mg/kg dose of verteporfin caused vascular shutdown in 12 out of 14 blood vessels observed within 60 min after PDT, we analyzed the relationship among vessel diameter, blood cell velocity and the time taken to reach zero blood flow. Figure 3 indicates no significant correlation between vessel diameter and blood cell velocity ($p=0.819$). Also there was no correlation between vessel diameter and the time taken to zero blood flow ($p=0.246$). However, a strong correlation was found between the initial blood cell velocity and the time taken to reach zero blood cell velocity ($p=0.007$).

Fluorescence images of 2,000 kDa FITC-dextran and 155 kDa TRITC-dextran were shown in Fig. 4 to illustrate the extravasation of macromolecules after treatments. Average fluorescence intensities of 2,000 kDa FITC-dextran and 155 kDa TRITC-dextran in ROIs were measured and shown

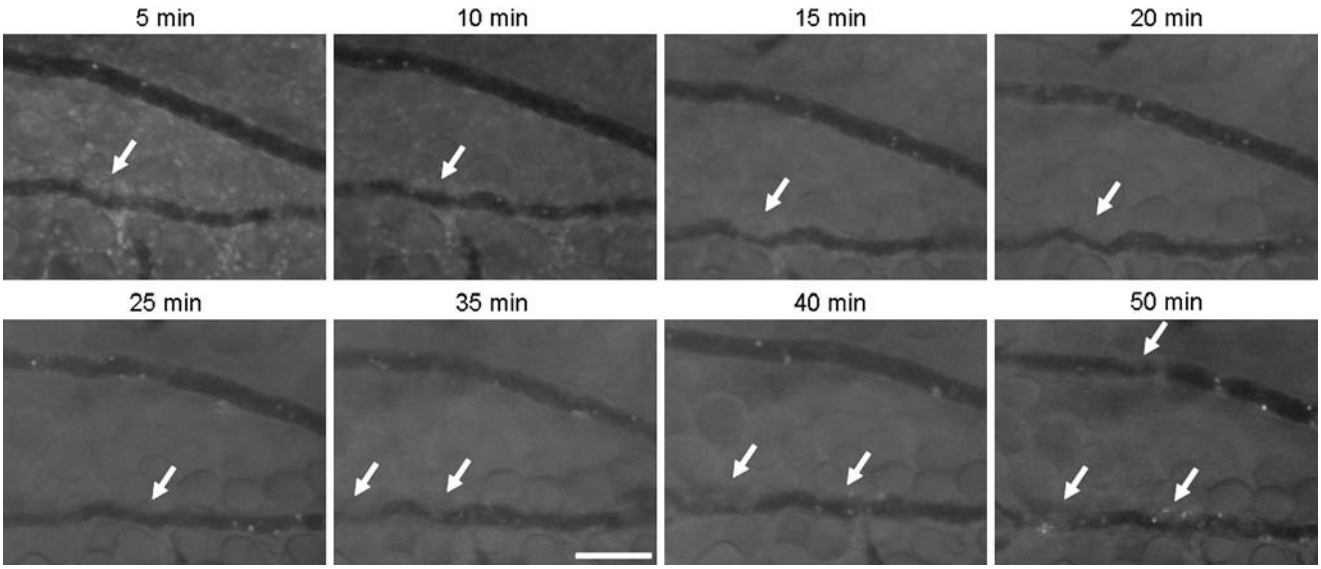

Fig. 1. Thrombus formation after PDT with verteporfin. The MatLyLu tumors were treated with 50 J/cm^2 light dose at 15 min after i.v. injection of 0.5 mg/kg dose of verteporfin. Tumor blood vessels were continuously imaged by intravital fluorescence microscopy showing the formation of thrombi (indicated by *arrows*) that caused progressive vessel lumen obstruction and ultimately vascular shutdown at 50 min after treatment. Bar=100 um.

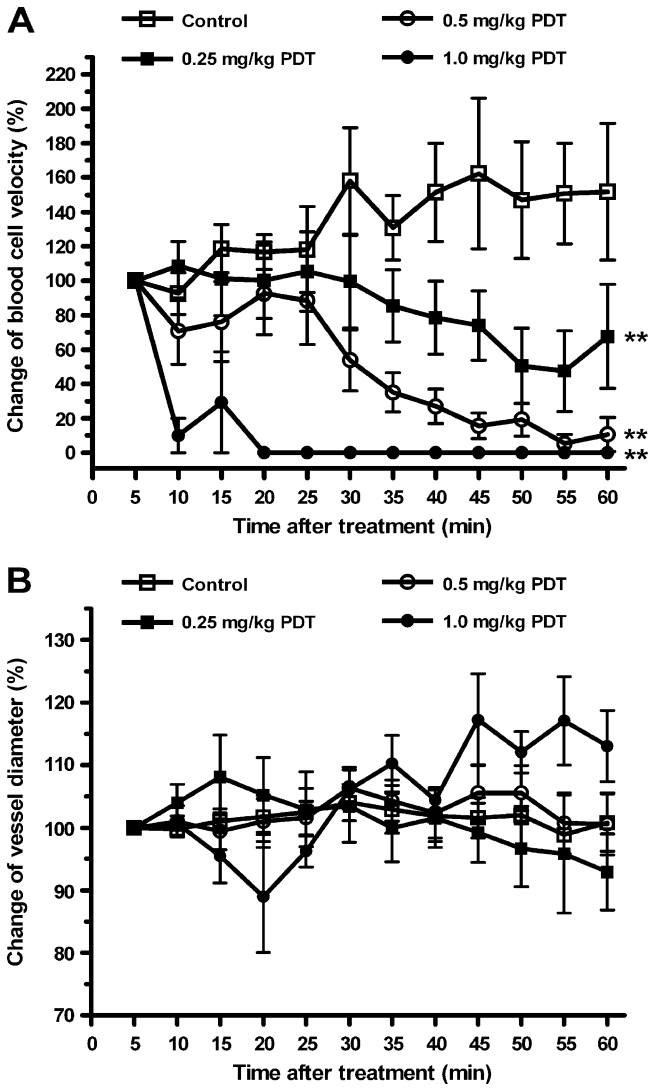

Fig. 2. Effects of PDT with verteporfin on blood cell velocity (**A**) and blood vessel diameter (**B**). The MatLyLu tumors were treated with 50 J/cm^2 light dose at 15 min after i.v. injection of 0.25, 0.5 or 1.0 mg/kg doses of verteporfin. Control tumors received no treatment. Blood cell velocity and vessel diameter were continuously measured every 5 min for up to 60 min after treatment by intravital fluorescence microscopy. Each data point represents the mean of 4–12 blood vessels and is expressed as a percentage of the 5 min point value. Bars indicate the standard error. Compared to the control, $^{**}p<0.01$.

in Fig. 5. The extravasation of 2,000 kDa FITC-dextran (Fig. 5A) and 155 kDa TRITC-dextran (Fig. 5B) led to significant increase in fluorescence intensity in untreated control tumors ($p<0.05$). Compared to untreated control tumors, PDT with 0.25 mg/kg dose of verteporfin significantly enhanced the extravasation of 2,000 kDa FITC-dextran in tumor tissues ($p<0.01$) while PDT with both 0.5 and 1.0 mg/kg doses of verteporfin had no significant effect on FITC-dextran extravasation ($p>0.05$). Both 0.25 and 0.5 mg/kg doses of verteporfin-PDT caused significant increase in the extravasation of 155 kDa TRITC-dextran compared to control tumors ($p<0.01$). But there was no significant difference between 0.25 and 0.5 mg/kg dose PDT treatments in affecting 155 kDa TRITC-dextran extravasation ($p>0.05$). PDT with 1.0 mg/kg dose of verteporfin induced an initial decrease in the fluorescence of 155 kDa TRITC-dextran. It is not clear what caused this decrease in the TRITC fluorescence, which was not observed in the corresponding FITC channel. The fluorescence of 155 kDa TRITC-dextran recovered after the initial decrease. Overall no significant difference was found between 1.0 mg/kg verteporfin-PDT and untreated control tumors in the TRITC-dextran extravasation over the 60 min period ($p>0.05$).

The AUC of fluorescence intensity–time curve was calculated to estimate tumor uptake of fluorochrome-labeled dextrans during the 60 min period (Fig. 6). Among three different doses of PDT treatments, only PDT with 0.25 mg/kg dose of verteporfin caused significant increase in tumor accumulation of 2,000 kDa FITC-dextran compared to control tumors ($p<0.05$). However, both 0.25 and 0.5 mg/kg doses of PDT significantly enhanced tumor accumulation of 155 kDa TRITC-dextran. Tumor uptake of 155 kDa TRITC-dextran was significantly higher than that of 2,000 kDa FITC-dextran after either 0.25 or 0.5 mg/kg PDT treatment ($p<0.01$). The 1.0 mg/kg dose PDT appeared to induce a decrease in tumor uptake of 155 kDa TRITC-dextran compared to control tumors, but this was not statistically significant ($p>0.05$).

DISCUSSION

Since tumor vasculature serves to provide blood supply to tumor tissues and regulate substance exchange between blood and tumor interstitial fluid (1), it is important to understand how a tumor vascular disrupting therapy affects these two key vascular functions. In the present study, we used intravital microscopy to analyze changes in tumor vascular perfusion and macromolecule extravasation after verteporfin-mediated photodynamic vascular targeting therapy in the orthotopic MatLyLu rat prostate tumor model. Based on our previous study that PDT with 0.25 mg/kg dose of verteporfin increases macromolecule extravasation and

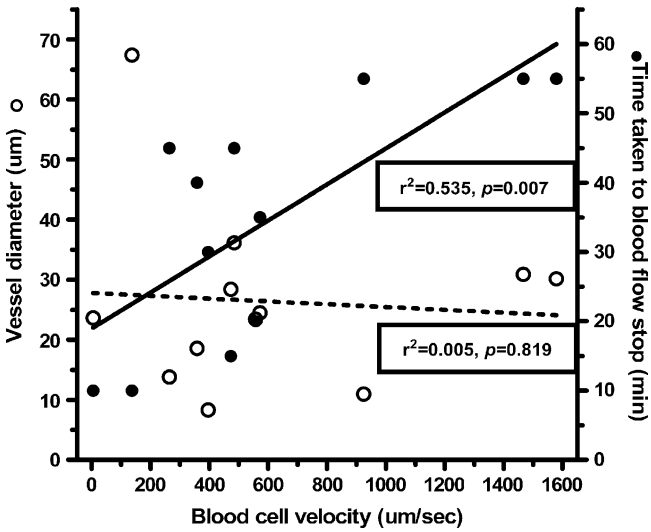

Fig. 3. Relationship between blood cell velocity and the time taken to reach zero blood flow after PDT with verteporfin. A significant correlation was found between the initial blood cell velocity and the time taken to zero blood cell velocity ($p=0.007$) after PDT with 0.5 mg/kg dose of verteporfin. The correlation between vessel diameter and blood cell velocity was not significant ($p=0.819$).

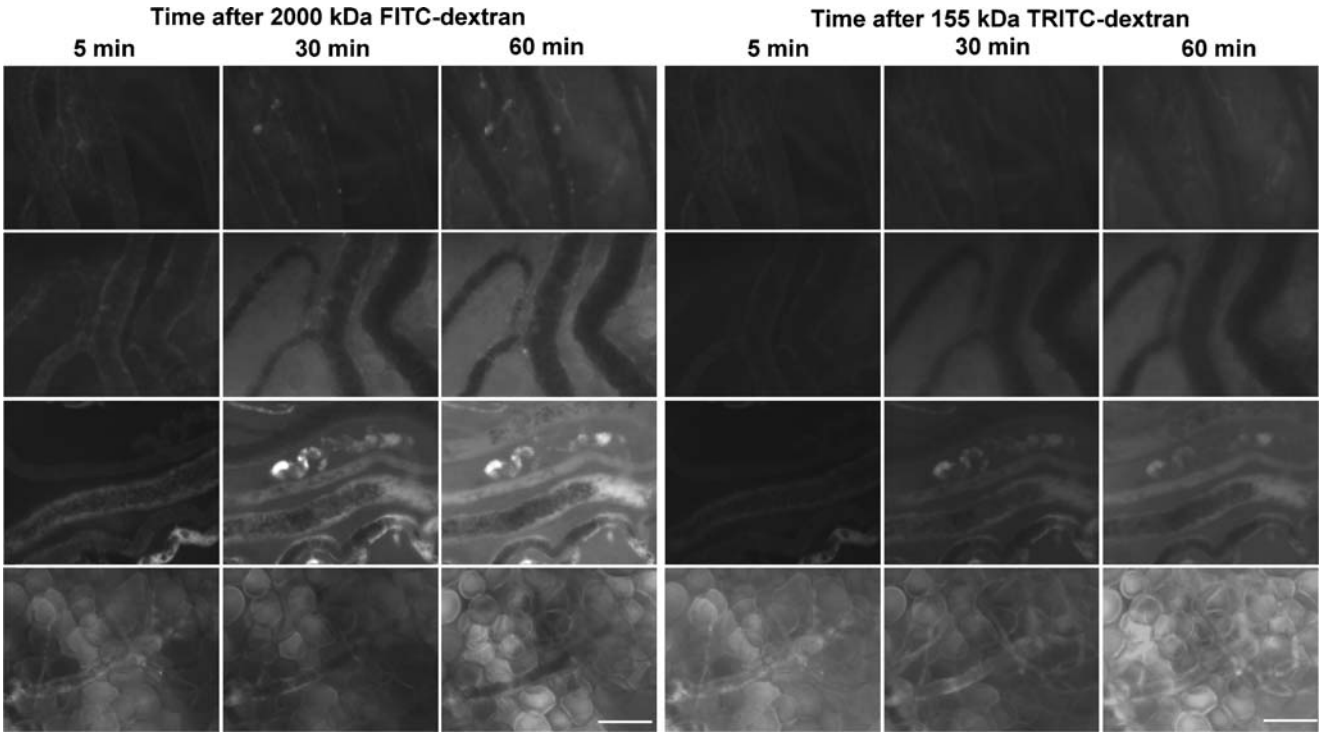

Fig. 4. Fluorescence images of 2,000 kDa FITC-dextran and 155 kDa TRITC-dextran at 5, 30 and 60 min after treatments. The MatLyLu tumors were treated with 50 J/cm^2 light dose at 15 min after i.v. injection of 0.25, 0.5 or 1.0 mg/kg doses of verteporfin. Control tumors received no treatment. Animals were i.v. injected with 2,000 kDa FITC-dextran and 155 kDa TRITC-dextran immediately after treatment and tumors were imaged with intravital fluorescence microcopy. *Top panel* control; *second panel* 0.25 mg/kg verteporfin-PDT; *third panel* 0.5 mg/kg verteporfin-PDT; *fourth panel* 1.0 mg/kg verteporfin-PDT. Bar=100 um.

induces tumor necrosis (9), we chose to examine two higher verteporfin doses (0.5 and 1.0 mg/kg) together with 0.25 mg/kg dose in this study. Our results demonstrate that PDT with verteporfin caused significant reduction in blood perfusion and an increase in the extravasation of dextran molecules. But the effects of PDT on blood perfusion and substance extravasation followed a reverse dose-dependence.

As expected, PDT with a higher dose of verteporfin was more effective in inducing blood flow reduction than a lower dose of verteporfin-PDT (Fig. 2). Similar to the previous studies (9,14,15), thrombus formation was found to contribute to PDT-induced vascular perfusion disruption. Stable thrombi formed inside vessel lumen caused blood flow reduction and even complete vascular occlusion. Even though vessel constriction was indeed observed in some blood vessels, vessel constriction in overall did not appear to play a major role in verteporfin-mediated vascular disruption, which has been reported to be involved in PDT with another photosensitizer Photofrin (16). Figure 2 indicates that no significant vessel size change was found after all three different doses of PDT treatments. This simply suggests the complexity of vessel response to PDT because, depending on the release of vasoactive substances with opposite effects on vessel size and spontaneous vessel response to tissue hypoxia, temperature and other microenvironment factors, both vessel constriction and dilation can happen at different time after verteporfin-PDT. These results are in agreement with those of Fingar *et al.* who reported that PDT with verteporfin had no significant effect on vessel diameter in a rat chondrosarcoma tumor model (15).

The mechanism underlying thrombus formation induced by photodynamic vascular targeting therapy is complicated and not yet clear. Reactive oxygen species generated intravascularly after PDT likely cause damage to multiple targets such as red blood cells, platelets and endothelial cells, which in turn leads to the activation of haemostatic cascades and results in thrombus formation (17,18). Endothelial damage plays an important role in initiating this cascade. As shown in the previous study, we have found a rapid endothelial cell microtubule depolymerization and endothelial cell contraction following verteporfin-PDT (9). Since endothelial cells form an interface between the blood and underneath tissue, these endothelial morphological changes lead to the exposure of tissue extracellular matrix to circulating blood, which causes blood cell adherence to the damaged endothelial cells via activating platelets and polymorphonuclear leukocytes (19,20). This might explain intravital microscopic observations that thrombi induced by verteporfin-PDT often started from endothelial sites and gradually increased in size, ultimately leading to blood vessel occlusion (Fig. 1).

Tumor blood vessels exhibited heterogeneity in response to PDT-induced perfusion disruption (21). By examining the response of each individual vessel to PDT, it is possible to identify the determinants that contribute to vascular response heterogeneity, which may help to find ways to enhance vascular response to PDT. Our data indicate that blood flow velocity was an important parameter in determining vascular response to PDT. Vessels with higher flow velocity were more resistant to PDT-induced vascular shutdown (Fig. 3). This is likely because high flow velocity was not conducive to

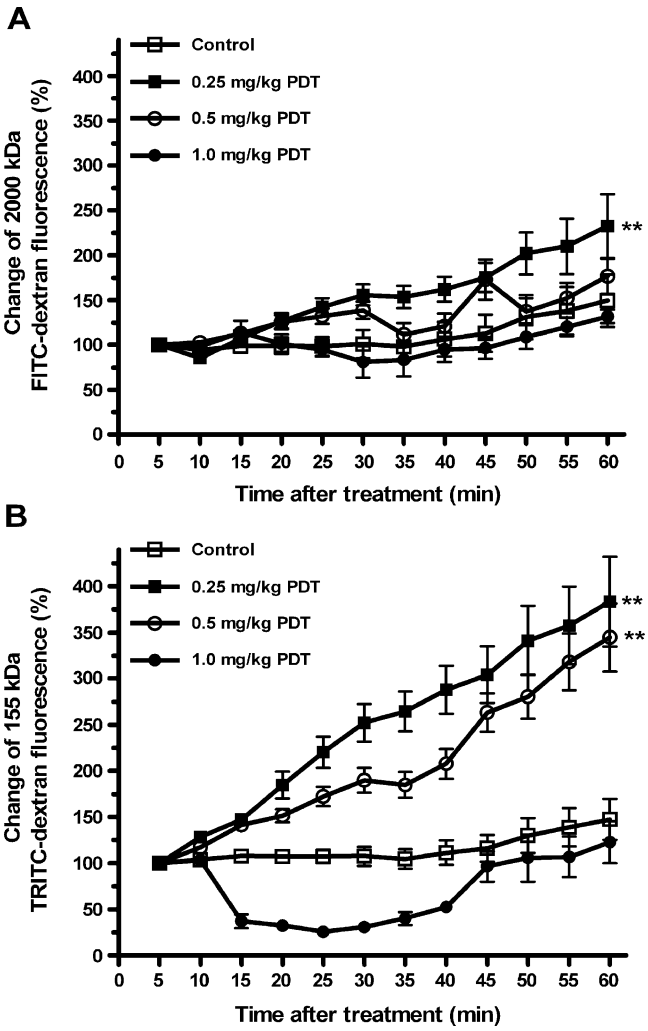

Fig. 5. Effects of PDT with verteporfin on the extravasation of 2,000 kDa FITC-dextran (**A**) and 155 kDa TRITC-dextran (**B**). The MatLyLu tumors were treated with 50 J/cm^2 light dose at 15 min after i.v. injection of 0.25, 0.5 or 1.0 mg/kg doses of verteporfin. Control tumors received no treatment. Animals were i.v. injected with 2,000 kDa FITC-dextran and 155 kDa TRITC-dextran immediately after treatment and tumors were imaged with intravital fluorescence microcopy. Fluorescence intensities of dextran molecules in the ROIs were continuously measured every 5 min for up to 60 min after treatment. Each data point represents the mean of 4–29 ROIs and is expressed as a percentage of the 5 min point value. *Bars* indicate the standard error. Compared to the control, $^{**}p<0.01$.

thrombus formation and able to push some already formed thrombi into circulation, which resumes blood perfusion function. Emboli were indeed commonly observed in blood vessels treated with a low dose of PDT and in vessels with fast blood flow in this study. A previous study demonstrates that tumor areas with low oxygen partial pressure (pO_2) have more rapid decrease in pO_2 level after verteporfin-PDT than areas with high pO_2 (22). Since it is very possible that tumor areas with low pO_2 also have low blood flow, the faster drop of tumor pO_2 in low pO_2 tumor areas than in high pO_2 tumor areas after PDT is likely because PDT induces a more rapid vascular shutdown in slow-flow vessels than in high-flow vessels. These results suggest that photodynamic vascular targeting therapy needs to be improved for targeting blood vessels with high blood flow. On the other hand, because tumor blood vessels generally have slower flow rate than normal vessels (23), this finding might explain why tumor vessels are more sensitive to vascular targeting PDT than normal vessels, which has been observed in the previous study (24).

Since vascular barrier is dependent upon endothelial tight junctions (25), another consequence of PDT-induced endothelial cell morphological change is the formation of inter-endothelial cell gaps, which disrupts vascular barrier. As shown in the present study, the extravasation and accumulation of high molecular weight dextran in tumor tissues were significantly increased as a result of vascular permeability increase after verteporfin-PDT. However, compared to the PDT effect on tumor perfusion, the effect of verteporfin-PDT on dextran delivery followed a reverse dose dependence. PDT with a lower dose of verteporfin was more effective in enhancing the extravasation and accumulation of dextran molecules in tumor tissues than a higher dose of verteporfin-PDT. This inverse dose dependence is likely due to the fact that PDT with a higher dose of verteporfin (e.g. 1.0 mg/kg) induced rapid vascular shutdown (Fig. 2), which prevented dextran molecules from being delivered to tumor tissues, while a lower dose verteporfin-PDT (e.g. 0.25 or 0.5 mg/kg) was able to maintain blood perfusion for sometime, which allowed continuous extravasation and accumulation of dextran molecules into the tumor tissue. These results suggest the importance of maintaining tumor perfusion in drug delivery enhancement by using a vascular targeted modality.

Our data also demonstrate that the enhancement of dextran delivery induced by verteporfin-PDT was dependent upon dextran molecular weight. Dextran with a lower molecular weight (155 kDa) exhibited a higher tumor extravasation and uptake than a higher molecular weight dextran (2,000 kDa) after both 0.25 and 0.5 mg/kg doses of PDT treatments. Since it has been known that tumor vascular permeability (26) and the transport of molecules in tumor interstitial area (27) decrease with the increase of molecular weight, the limited enhancement seen in the delivery of 2,000 kDa dextran was likely because it has a lower vascular permeability and slower diffusion in tumor interstitial area than the 155 kDa dextran.

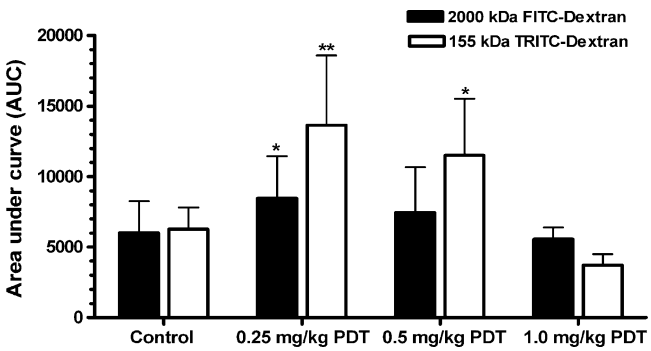

Fig. 6. Effects of PDT with verteporfin on the accumulation of 2,000 kDa FITC-dextran and 155 kDa TRITC-dextran in tumor tissues. The AUC of fluorescence intensity-time curve, as described in the legend of Fig. 5, was calculated to represent the tumor accumulation of dextran molecules. Compared to the control, $^{*}p<0.05$, $^{**}p<0.01$.

This study implies that, although photodynamic vascular targeting therapy with verteporfin may be used for both tumor destruction and drug delivery enhancement, optimal PDT conditions should be tailored to different therapeutic applications. PDT with a higher dose of verteporfin (e.g. 1.0 mg/kg) might be more appropriate for tumor eradication as a rapid and extensive vascular shutdown might be able to maximize tumor cell killing by oxygen and nutrients deprivation. We have found that PDT with 0.25 mg/kg dose of verteporfin causes substantial tumor necrosis. It remains to be determined whether PDT with a higher dose of verteporfin will lead to more tumor necrosis. For primarily enhancing the delivery of other therapeutic agents, PDT with a lower dose of verteporfin (e.g. 0.25 mg/kg) is likely preferred because it can obtain optimal drug tumor accumulation by maintaining tumor perfusion after treatment, as shown in the present and previous (9) study. PDT has been proposed to enhance the delivery of anticancer agent (8). Strategies such as illumination with low light doses and low dose rates (8) or in combination with anti-coagulants (28) also work through preserving tumor perfusion to obtain an enhanced drug delivery to tumor tissues. However, for most cancer combination therapies, PDT with an intermediate dose of verteporfin (e.g. 0.5 mg/kg) is likely to be a practical choice because this treatment can cause considerable tumor perfusion disruption and some effect of drug delivery enhancement, as demonstrated in the present study. Combination of intermediate dose PDT with anticancer drug therapy is more likely to achieve synergistic effect.

In conclusion, we found that photodynamic vascular targeting with verteporfin disrupted tumor perfusion by inducing thrombus formation, and enhanced tumor accumulation of high molecular weight dextrans by increasing vascular permeability. However, effects of PDT on blood perfusion and accumulation of dextran molecules followed a reverse dose dependence. A higher dose of verteporfin PDT was more effective in inducing perfusion disruption, but less effective in enhancing dextran accumulation. A lower dose of verteporfin PDT was favorable for drug delivery enhancement by maintaining tumor perfusion. Dextran with a lower molecular weight (155 kDa) obtained a higher tumor accumulation than a higher molecular weight dextran (2,000 kDa). These findings are important for optimizing PDT conditions as a vascular disrupting therapy or a modality for drug delivery enhancement.

ACKNOWLEDGEMENTS

This work is supported by Department of Defense (DOD) Grant W81XWH-06-1-0148 and Lindback Foundation. The authors would like to gratefully acknowledge Dr. Brian Pogue for reading the manuscript and QLT Inc. for providing photosensitizer verteporfin.

REFERENCES

1. C. Bouzin and O. Feron. Targeting tumor stroma and exploiting mature tumor vasculature to improve anti-cancer drug delivery. *Drug Resist. Updat.* **10**:109–20 (2007).
2. D. W. Siemann, M. C. Bibby, G. G. Dark, A. P. Dicker, F. A. Eskens, M. R. Horsman, D. Marme, and P. M. Lorusso. Differentiation and definition of vascular-targeted therapies. *Clin. Cancer Res*. **11**:416–20 (2005).
3. F. Yuan. Transvascular drug delivery in solid tumors. *Semin. Radiat. Oncol*. **8**:164–75 (1998).
4. G. P. van Nieuw Amerongen and V. W. van Hinsbergh. Targets for pharmacological intervention of endothelial hyperpermeability and barrier function. *Vasc. Pharmacol*. **39**:257–72 (2002).
5. T. J. Dougherty, C. J. Gomer, B. W. Henderson, G. Jori, D. Kessel, M. Korbelik, J. Moan, and Q. Peng. Photodynamic therapy. *J. Natl. Cancer Inst*. **90**:889–905 (1998).
6. D. E. Dolmans, D. Fukumura, and R. K. Jain. Photodynamic therapy for cancer. *Nat. Rev. Cancer.* **3**:380–7 (2003).
7. B. Chen, B. W. Pogue, P. J. Hoopes, and T. Hasan. Vascular and cellular targeting for photodynamic therapy. *Crit. Rev. Eukaryot Gene Expr.* **16**:279–305 (2006).
8. J. W. Snyder, W. R. Greco, D. A. Bellnier, L. Vaughan, and B. W. Henderson. Photodynamic therapy: a means to enhanced drug delivery to tumors. *Cancer Res*. **63**:8126–31 (2003).
9. B. Chen, B. W. Pogue, J. M. Luna, R. L. Hardman, P. J. Hoopes, and T. Hasan. Tumor vascular permeabilization by vascular-targeting photosensitization: effects, mechanism, and therapeutic implications. *Clin. Cancer Res*. **12**:917–23 (2006).
10. R. K. Jain, L. L. Munn, and D. Fukumura. Dissecting tumour pathophysiology using intravital microscopy. *Nat. Rev. Cancer* **2**:266–76 (2002).
11. T. R. Tennant, H. Kim, M. Sokoloff, and C. W. Rinker-Schaeffer. The Dunning model. *Prostate* **43**:295–302 (2000).
12. B. Chen, B. W. Pogue, X. Zhou, J. A. O'Hara, N. Solban, E. Demidenko, P. J. Hoopes, and T. Hasan. Effect of tumor host microenvironment on photodynamic therapy in a rat prostate tumor model. *Clin. Cancer Res*. **11**:720–7 (2005).
13. B. Chen, B. W. Pogue, P. J. Hoopes, and T. Hasan. Combining vascular and cellular targeting regimens enhances the efficacy of photodynamic therapy. *Int. J. Radiat. Oncol. Biol. Phys*. **61**:1216–26 (2005).
14. U. Schmidt-Erfurth and T. Hasan. Mechanisms of action of photodynamic therapy with verteporfin for the treatment of age-related macular degeneration. *Surv. Ophthalmol*. **45**:195–214 (2000).
15. V. H. Fingar, P. K. Kik, P. S. Haydon, P. B. Cerrito, M. Tseng, E. Abang, and T. J. Wieman. Analysis of acute vascular damage after photodynamic therapy using benzoporphyrin derivative (BPD). *Br. J. Cancer.* **79**:1702–8 (1999).
16. V. H. Fingar, T. J. Wieman, S. A. Wiehle, and P. B. Cerrito. The role of microvascular damage in photodynamic therapy: the effect of treatment on vessel constriction, permeability, and leukocyte adhesion. *Cancer Res*. **52**:4914–21 (1992).
17. V. H. Fingar. Vascular effects of photodynamic therapy. *J. Clin. Laser Med. Surg*. **14**:323–8 (1996).
18. B. Krammer. Vascular effects of photodynamic therapy. *Anticancer Res*. **21**:4271–7 (2001).
19. W. J. de Vree, M. C. Essers, H. S. de Bruijn, W. M. Star, J. F. Koster, and W. Sluiter. Evidence for an important role of neutrophils in the efficacy of photodynamic therapy *in vivo*. *Cancer Res*. **56**:2908–11 (1996).
20. W. J. de Vree, A. N. Fontijne-Dorsman, J. F. Koster, and W. Sluiter. Photodynamic treatment of human endothelial cells promotes the adherence of neutrophils *in vitro*. *Br. J. Cancer.* **73**:1335–40 (1996).
21. T. M. Busch. Local physiological changes during photodynamic therapy. *Lasers Surg. Med*. **38**:494–9 (2006).
22. B. W. Pogue, R. D. Braun, J. L. Lanzen, C. Erickson, and M. W. Dewhirst. Analysis of the heterogeneity of pO2 dynamics during photodynamic therapy with verteporfin. *Photochem. Photobiol.* **74**:700–6 (2001).
23. D. Fukumura and R. K. Jain. Tumor microenvironment abnormalities: causes, consequences, and strategies to normalize. *J. Cell Biochem*. **101**:937–49 (2007).
24. F. Borle, A. Radu, C. Fontolliet, H. van den Bergh, P. Monnier, and G. Wagnieres. Selectivity of the photosensitiser Tookad for photodynamic therapy evaluated in the Syrian golden hamster cheek pouch tumour model. *Br. J. Cancer.* **89**:2320–6 (2003).
25. G. Bazzoni. Endothelial tight junctions: permeable barriers of the vessel wall. *Thromb Haemost*. **95**:36–42 (2006).

26. M. R. Dreher, W. Liu, C. R. Michelich, M. W. Dewhirst, F. Yuan, and A. Chilkoti. Tumor vascular permeability, accumulation, and penetration of macromolecular drug carriers. *J. Natl. Cancer Inst.* **98**:335–44 (2006).
27. A. Pluen, Y. Boucher, S. Ramanujan, T. D. McKee, T. Gohongi, E. di Tomaso, E. B. Brown, Y. Izumi, R. B. Campbell, D. A. Berk, and R. K. Jain. Role of tumor–host interactions in interstitial diffusion of macromolecules: cranial *vs.* subcutaneous tumors. *Proc. Natl. Acad. Sci. U S A*. **98**:4628–33 (2001).
28. E. Debefve, B. Pegaz, J. P. Ballini, Y. N. Konan, and H. van den Bergh. Combination therapy using aspirin-enhanced photodynamic selective drug delivery. *Vasc. Pharmacol.* **46**:171–80 (2007).

Int. J. Cancer: **123,** 695–701 (2008)

Disparity between prostate tumor interior *versus* peripheral vasculature in response to verteporfin-mediated vascular-targeting therapy

Bin Chen[1,2]*, Curtis Crane[3], Chong He[1], David Gondek[4], Priyanka Agharkar[1], Mark D. Savellano[3,5], P. Jack Hoopes[3,5] and Brian W. Pogue[3,5,6]

[1]*Department of Pharmaceutical Sciences, Philadelphia College of Pharmacy, University of the Sciences in Philadelphia, Philadelphia, PA*
[2]*Department of Radiation Oncology, University of Pennsylvania, Philadelphia, PA*
[3]*Department of Surgery, Dartmouth Medical School, Lebanon, NH*
[4]*Department of Immunology, Dartmouth Medical School, Lebanon, NH*
[5]*Thayer School of Engineering, Dartmouth College, Hanover, NH*
[6]*Wellman Center for Photomedicine, Massachusetts General Hospital, Department of Dermatology, Harvard Medical School, Boston, MA*

Photodynamic therapy (PDT) is a light-based cancer treatment modality. Here we employed both *in vivo* and *ex vivo* fluorescence imaging to visualize vascular response and tumor cell survival after verteporfin-mediated PDT designed to target tumor vasculature. EGFP-MatLyLu prostate tumor cells, transduced with EGFP using lentivirus vectors, were implanted in athymic nude mice. Immediately after PDT with different doses of verteporfin, tumor-bearing animals were injected with a fluorochrome-labeled albumin. The extravasation of fluorescent albumin along with tumor EGFP fluorescence was monitored noninvasively with a whole-body fluorescence imaging system. *Ex vivo* fluorescence microscopy was performed on frozen sections of tumor tissues taken at different times after treatment. Both *in vivo* and *ex vivo* imaging demonstrated that vascular-targeting PDT with verteporfin significantly increased the extravasation of fluorochrome-labeled albumin in the tumor tissue, especially in the tumor periphery. Although PDT induced substantial vascular shutdown in interior blood vessels, some peripheral tumor vessels were able to maintain perfusion function up to 24 hr after treatment. As a result, viable tumor cells were typically detected in the tumor periphery in spite of extensive tumor cell death. Our results demonstrate that vascular-targeting PDT with verteporfin causes a dose- and time-dependent increase in vascular permeability and decrease in blood perfusion. However, compared to the interior blood vessels, peripheral tumor blood vessels were found less sensitive to PDT-induced vascular shutdown, which was associated with subsequent tumor recurrence in the tumor periphery.

Key words: photodynamic therapy (PDT); verteporfin; vascular targeting; fluorescence imaging; vascular permeability; tumor perfusion; enhanced green fluorescence protein (EGFP); prostate tumor model

Photodynamic therapy (PDT) induces tumor destruction through a photochemical reaction involving a photosensitizer, light of a specific wavelength matching the absorption of the photosensitizer and molecular oxygen.[1] Singlet oxygen, a product of this photochemical reaction, causes oxidative damage to target cells and tissues and is the primary reactive oxygen species responsible for the biological effects of PDT.[2] Although direct tumor cytotoxicity and immune responses are involved as well, damage to the tumor vasculature has been shown to contribute significantly to the overall PDT effect of most photosensitizers.[3]

Verteporfin (the lipid-formulation of benzoporphyrin derivative monoacid ring A) is a photosensitizer that is currently approved for the treatment of age-related macular degeneration (AMD).[4] We have shown previously that the dynamic distribution of verteporfin is predominantly intravascular at 15 min after intravenous injection and becomes mainly extravascular at 3 hr after injection.[5] Based on this pharmacokinetic property, preferential tumor vascular targeting can be achieved by illumination at 15 min after verteporfin administration. We have been exploring this passive vascular targeting principle for the treatment of prostate tumors. Intravital fluorescence microscopy studies in the MatLyLu rat prostate tumor model has demonstrated that vascular-targeting PDT with verteporfin induces vascular permeability increase and thrombus formation, which ends in vascular shutdown and tumor necrosis.[6] These results indicate that vascular-targeting PDT using verteporfin can be used for the management of localized prostate cancer.

Because vascular damage is the dominant effect of PDT, especially in the case of vascular-targeting PDT, it is important to study in detail how photosensitization modifies vascular functions. Most studies on PDT-induced tumor vascular changes have been done on excised tumor specimens after sacrificing the animals. Although they have been valuable in revealing microscopic details, such studies are only able to provide snap-shot information on each individual animal. To obtain longitudinal information in a single animal, noninvasive imaging techniques are necessary to examine vessel functional changes after PDT. Imaging modalities such as laser Doppler perfusion imaging,[7,8] diffuse correlation spectroscopy,[9] laser speckle imaging,[10,11] optical coherence tomography[12] and ultrasonography[13] have all been shown to be useful techniques for monitoring tumor blood flow dynamics noninvasively after PDT. Moreover, noninvasive imaging using contrast agents allows one to follow perfusion changes and also provides real-time information regarding vascular permeability. For instance, angiography with fluorescent dyes such as fluorescein or indocyanine green is routinely used to examine vessel leakage and occlusion in AMD patients treated with PDT.[14] Changes in tumor perfusion and vascular permeability after PDT have also been studied with contrast-enhanced MRI.[15,16]

Because of its high sensitivity and versatility, *in vivo* fluorescence imaging is able to provide both macroscopic and microscopic longitudinal data in individual animals, which cannot be obtained in other ways.[17–19] In this study, we used an *in vivo* whole-body fluorescence imaging system to monitor vascular response and tumor cell survival in an EGFP-expressing prostate tumor model following treatment with verteporfin-PDT. Moreover, we compared the *in vivo* tumor imaging results with the *ex vivo* fluorescence microscopy of frozen tumor sections. Our results indicate that the vascular response to vascular-targeting PDT is clearly different between tumor interior vessels and peripheral blood vessels.

Grant sponsor: Department of Defense (DOD) Prostate Cancer Research; Grant number: W81XWH-06-1-0148; Grant sponsor: Lindback Foundation.

***Correspondence to:** Department of Pharmaceutical Sciences, Philadelphia College of Pharmacy, University of the Sciences in Philadelphia, 600 South 43rd Street, Philadelphia, PA 19104, USA Fax: 215-895-1161. E-mail: b.chen@usip.edu

Received 14 December 2007; Accepted after revision 1 February 2008
DOI 10.1002/ijc.23538
Published online 22 May 2008 in Wiley InterScience (www.interscience.wiley.com).

Material and methods

Production and titer of lentivirus

Lentiviral production was performed as previously described.[20] Briefly, we cotransfected pWPT-EGFP and third-generation packaging vectors into 293FT cells (Invitrogen Life Technologies) and collected culture supernatants after 48 and 72 hr of incubation in a 37°C and 5% CO_2 incubator. We recovered virus by ultracentrifugation (1.5 hr at 25,000 rpm) in a Beckman SW28 rotor and resuspended the virus pellet in 25 μl of Opt-MEM media (Invitrogen Life Technologies). Viral titers were determined by infecting 293FT cells with serial dilutions of concentrated lentivirus followed by flow cytometry analysis 48 hr later. Typical viral preparations yielded 5×10^8 transducing units/ml.

Tumor cells and lentiviral transduction

R3327-MatLyLu rat prostate cancer cells were maintained in the RPMI-1640 medium with glutamine (Mediatech, Herndon, VA) supplemented with 10% fetal bovine serum (HyClone, Logan, UT) and 100 units/ml penicillin–streptomycin (Mediatech) at 37°C in a 5% CO_2 incubator. For lentiviral transduction, the MatLyLu cells were infected with a multiplicity of infection of 50 and allowed to incubate overnight. Polybrene (8 μg/ml, Sigma) was used to facilitate lentiviral transduction. Supernatant was then removed after infection and replaced with complete RPMI-1640 growth medium. EGFP-transduced MatLyLu cells were examined with a fluorescence microscope at 48 hr after transduction. EGFP-MatLyLu cells were harvested, serial diluted and seeded in a 96-well plate with cell density of 1 cell per well. After incubation for 7 days at 37°C and 5% CO_2 atmosphere, the clone exhibiting the highest EGFP fluorescence intensity was selected and expanded for subsequent experiments.

Animals and tumor models

Male NCr athymic nude mice (4–5 weeks old, National Cancer Institute, Frederick, MD) were used throughout the study. Tumors were induced by subcutaneous injection of about 1×10^5 EGFP-MatLyLu tumor cells in the thigh region of mice. Tumors were used for experiments when they reached a size of 5–7 mm in diameter. All animal procedures were carried out according to a protocol approved by the Institutional Animal Care and Use Committee (IACUC).

Photosensitizer

Verteporfin (benzoporphyrin derivative (BPD) in a lipid-formulation) was obtained from QLT (Vancouver, Canada) as a gift. A stock saline solution of verteporfin was reconstituted according to the manufacturer's instructions and stored at 4°C in the dark.

PDT treatments

A diode laser system (High Power Devices, North Brunswick, NJ) at 690-nm wavelength was used for the irradiation of EGFP-MatLyLu tumors. The laser was coupled to an optical fiber with 600 μm core diameter and expanded to generate an 11-mm diameter illumination spot through a collimator. Animals were anesthetized with injection (i.p.) of a mixture of ketamine (90 mg/kg) and xylazine (9 mg/kg) and tumors were exposed to light with an irradiance of 50 mW/cm^2. Light intensity was measured with an optical power meter (Thorlabs, North Newton, NJ). Verteporfin was injected (i.v.) 15 min prior to light irradiation at a dose of 0.25 mg/kg.

Noninvasive tumor fluorescence imaging and image analysis

Tumor-bearing animals were i.v. injected with 20 mg/kg albumin labeled with tetramethylrhodamine isothiocyanate (TRITC-albumin, Sigma) immediately after PDT. EGFP-MatLyLu tumors were imaged with a noninvasive whole body fluorescence imaging system for the EGFP and TRITC signal before and at various times after treatment. The setup of this home-built broad beam imaging system has been described in detail in our previous paper.[21] Briefly, the system includes a filtered white light source for excitation and a SensiCamQE high performance digital CCD camera (The Cook Corp, Auburn Hills, MI) to capture fluorescence emission passing through an emission filter. We used a 470/20 nm excitation filter and a 520/20 nm emission filter for imaging tumor EGFP fluorescence and a 535/20 nm excitation filter and 590-nm long-pass emission filter for imaging the TRITC fluorescence. Camera settings were kept constant for the control and PDT-treated animals throughout the imaging process. Animals were anesthetized by inhalation of 1.5% isofluorane and imaged first for EGFP and then TRITC fluorescence without moving the animals. The EGFP and TRITC images were pseudocolored and superimposed to generate composite images.

A 2.5-mm diameter region of interest (ROI) was centered over tumor or tumor-adjacent normal tissue areas, and the average EGFP and TRITC fluorescence intensities in the ROI were quantified with NIH ImageJ software. The fluorescence intensity in tumor or tumor-adjacent tissues after PDT was normalized to its own pretreatment value in each animal, and the data from different animals in each group were pooled to generate response curves. To determine the TRITC-albumin distribution in relation to tumor EGFP fluorescence, a straight line was drawn through the tumor tissue on composite images and the corresponding green (EGFP) and red (TRITC) intensities were measured along the line.

Tumor tissue fluorescence microscopy

Tumor-bearing animals were i.v. injected with 20 mg/kg Hoechst (Sigma) as a vascular perfusion marker at different time points after treatment. Animals were euthanized within 1 min after injection and tumor tissues were excised and snap-frozen in isopentane precooled with liquid nitrogen. Frozen tumor sections with thickness of 10 μm were cut and examined under a Leica DMI6000B fluorescence microscope with appropriate filter sets for Hoechst (excitation: 360/40 nm; emission: 470/40 nm) and TRITC (excitation: 546/12 nm; emission: 600/40 nm).

Tumor volume measurement and tumor histology

Three-dimensional tumor sizes were measured regularly after treatment by caliper, and the tumor volume was calculated using the formula $\pi/6 \times$ tumor length $\times$ tumor width $\times$ tumor height. Animals were euthanized at various time points after treatment. Tumor tissues were excised and fixed in 4% formalin solution. Fixed tumor tissues were dehydrated and then embedded in paraffin. Tissue sections with thickness of 5 μm were cut and stained with H&E.

Statistical analysis

Students' 2-tailed *t*-test was used to calculate statistical differences between 2 groups and the significance was accepted at $p < 0.05$. Statistical analysis was carried out using GraphPad software (GraphPad, San Diego, CA).

Results

The extravasation of TRITC-albumin, as indicated by the increase in TRITC fluorescence, was imaged noninvasively with a whole-body fluorescence imaging system. Figure 1 shows the TRITC fluorescence images (red) merged with tumor EGFP fluorescence images (green) at different time points after vascular-targeting PDT with verteporfin. PDT caused an overall increase in the TRITC fluorescence and this was more pronounced in the peritumor area. PDT-induced TRITC-albumin extravasation appeared to be dose dependent because the 50 J/cm^2 light dose PDT caused a greater increase in the TRITC fluorescence compared to the 25 J/cm^2 light dose treatment.

The average TRITC fluorescence intensity in tumor and tumor-adjacent normal tissue ROIs was quantified with NIH ImageJ software. It was observed that the average TRITC fluorescence in

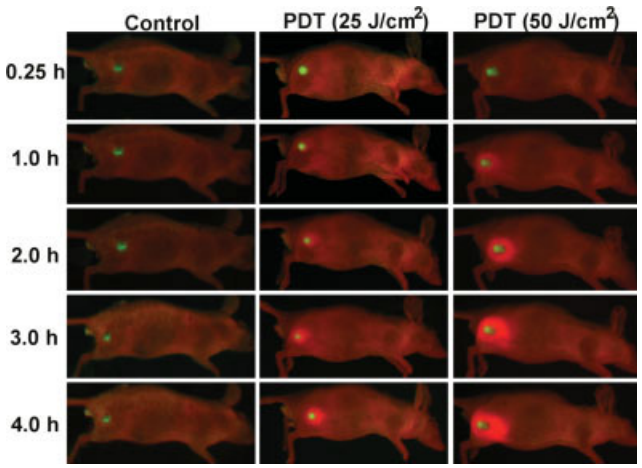

FIGURE 1 – *In vivo* fluorescence images of the TRITC-albumin extravasation and tumor EGFP fluorescence. The EGFP-MatLyLu tumors were illuminated with 25 or 50 J/cm^2 light at 15 min after i.v. injection of 0.25 mg/kg dose of verteporfin. Immediately after treatment, tumor-bearing animals were i.v. injected with 20 mg/kg TRITC-albumin and imaged at different times after injection with a whole-body fluorescence imaging system as described in the materials and methods. Control tumors received no treatment. The images shown are the merged image of TRITC (red) and EGFP (green) fluorescence images. [Color figure can be viewed in the online issue, which is available at www.interscience.wiley.com.]

tumor areas was about 20% lower than tumor-adjacent normal tissue areas presumably because higher blood volume in tumor tissues causes more TRITC fluorescence quenching than in normal tissues.[19] Both 25 and 50 J/cm^2 PDT treatments significantly increased the TRITC fluorescence intensity in tumor (Fig. 2*a*, $p < 0.05$) and tumor-adjacent tissues (Fig. 2*b*, $p < 0.05$). Fluorescence intensity increase started from 1-hr post-PDT treatments and reached a plateau at about 4 hr thereafter while untreated control tumors exhibited little change in fluorescence intensity over the same period of time. In both tumor and tumor-adjacent tissues, PDT with 50 J/cm^2 light dose induced a greater increase in the TRITC fluorescence intensity than the 25 J/cm^2 light dose ($p < 0.01$). The 25 J/cm^2 light dose PDT caused a similar increase (maximally about 1.5-fold increase) in the TRITC fluorescence intensity in both tumor and tumor-adjacent tissues ($p > 0.05$). The 50 J/cm^2 PDT caused significantly higher TRITC fluorescence increase in tumor-adjacent tissues (about 3-fold increase at peak) compared to tumor tissues (about 2-fold increase at peak, $p < 0.05$).

Changes in the average EGFP fluorescence intensity in tumor tissues were also quantified and are shown in Figure 2*c*. Both 25 and 50 J/cm^2 PDT treatments caused a significant decrease in tumor EGFP fluorescence at 1 hr after treatment ($p < 0.05$). After the initial decrease, there was no further decrease in tumor EGFP fluorescence intensity. Control tumors showed little change in the EGFP fluorescence during this 5-hr period.

Analysis of TRITC and corresponding EGFP intensity profiles indicated that the TRITC fluorescence intensity in tumor peripheral area was higher than in tumor interior area at 4 hr after injection of TRITC-albumin (Fig. 3). However, an opposite pattern was found in tumor EGFP intensity profiles with the higher intensity values detected in the tumor center. Both 25 and 50 J/cm^2 PDT treatments caused an overall increase in the TRITC intensity and decrease in tumor EGFP intensity. The increase in the TRITC intensity was found to be higher in the tumor periphery than in the tumor center.

To verify the whole-body fluorescence imaging results, we euthanized animals at 1, 4 and 24 hr after 50 J/cm^2 PDT treatment and excised tumor tissues for fluorescence microscopy. Hoechst dye was i.v. injected shortly before euthanizing animals to highlight functional blood vessels. As shown in Figure 4, tumor staining of Hoechst dye decreased significantly after vascular-targeting PDT with 50 J/cm^2 light dose compared to the control tumor, indicating a decrease in functional blood vessels. Moreover, functional

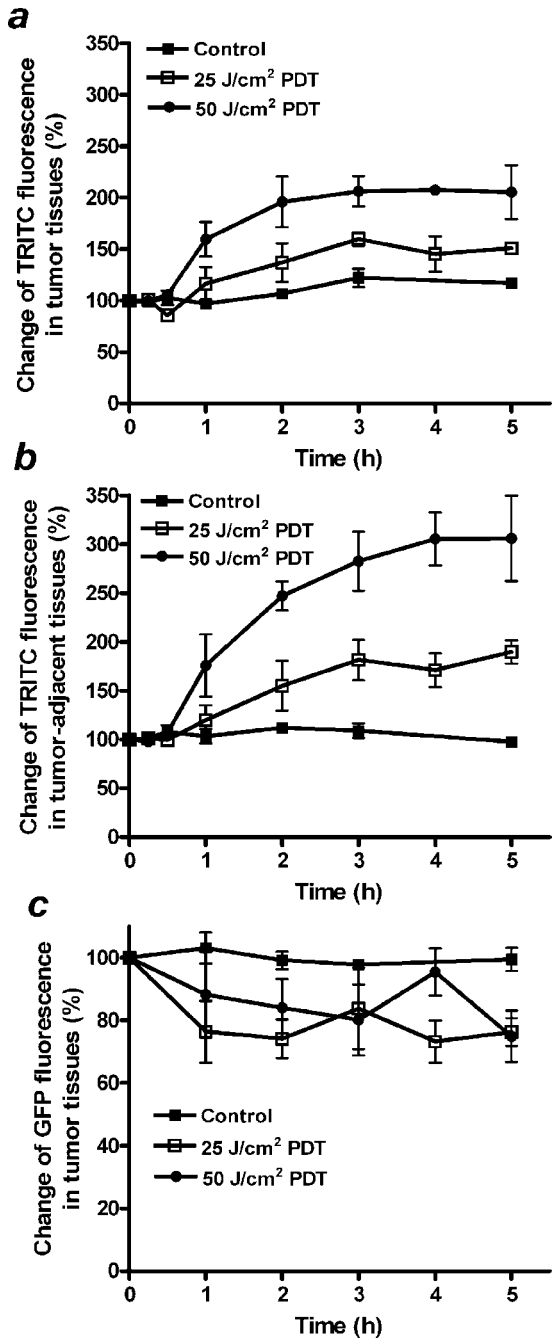

FIGURE 2 – *In vivo* fluorescence image analysis showing (*a*) changes of the TRITC-albumin fluorescence intensity in tumor tissues, (*b*) changes of the TRITC-albumin fluorescence intensity in tumor-adjacent tissues, and (*c*) changes of tumor EGFP fluorescence intensity after treatment. The EGFP-MatLyLu tumors were treated with vascular-targeting PDT and imaged with a whole-body fluorescence imaging system. The TRITC and EGFP fluorescence intensities were measured in a circular 2.5 mm diameter ROI placed over the tumor or tumor-adjacent area on the fluorescence images. The fluorescence intensity values after treatment in each animal were normalized to their own pretreatment values, which are displayed as 100% at 0 time point. Each group included 3 or 4 animals. Error bars represent the standard deviation.

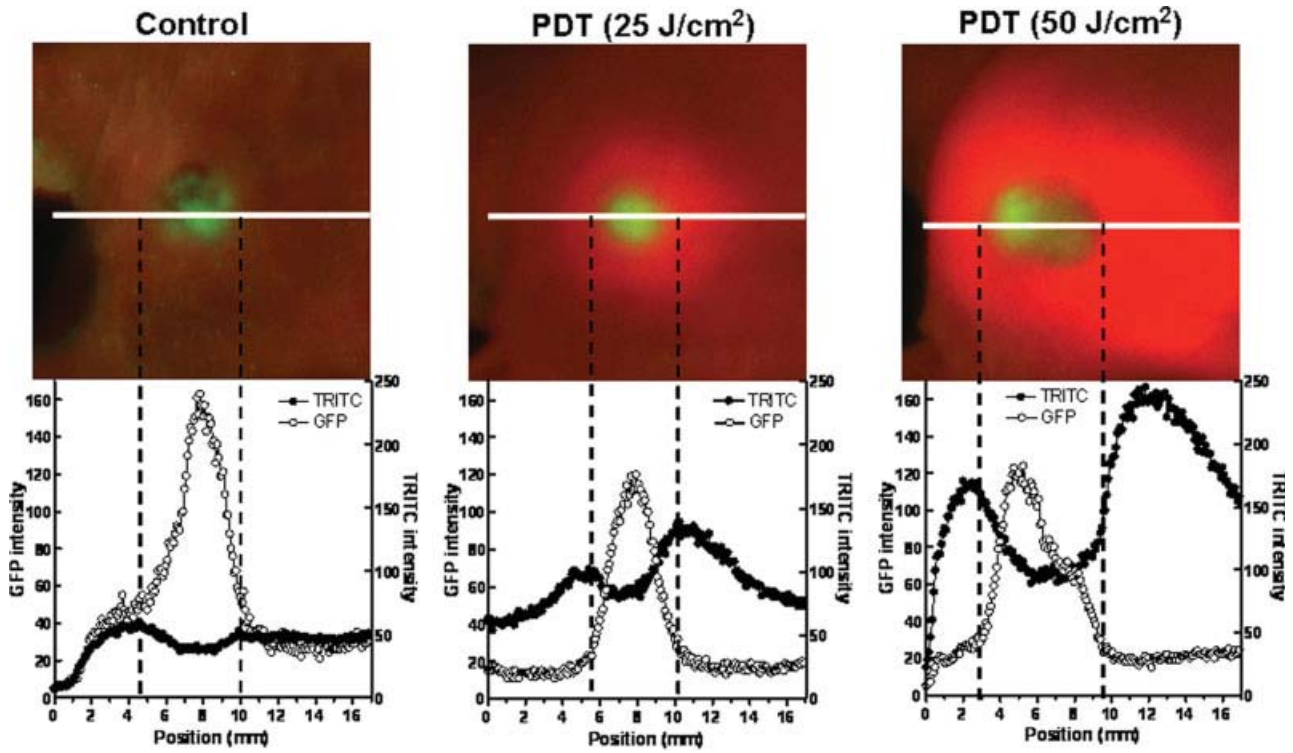

FIGURE 3 – *In vivo* fluorescence image analysis showing the TRITC-albumin accumulation in relation to tumor EGFP fluorescence intensity. The 4-hr-time-point images from Figure 1 were analyzed and shown here. A 17-mm line was drawn through the tumor tissue on each fluorescence image. Both TRITC-albumin and tumor EGFP fluorescence intensities were measured along the line and are shown in the figure. Dashed lines indicate the boundary of the tumor tissue. Note the opposite pattern between tumor TRITC-albumin accumulation and tumor EGFP fluorescence intensity profiles. [Color figure can be viewed in the online issue, which is available at www.interscience.wiley.com.]

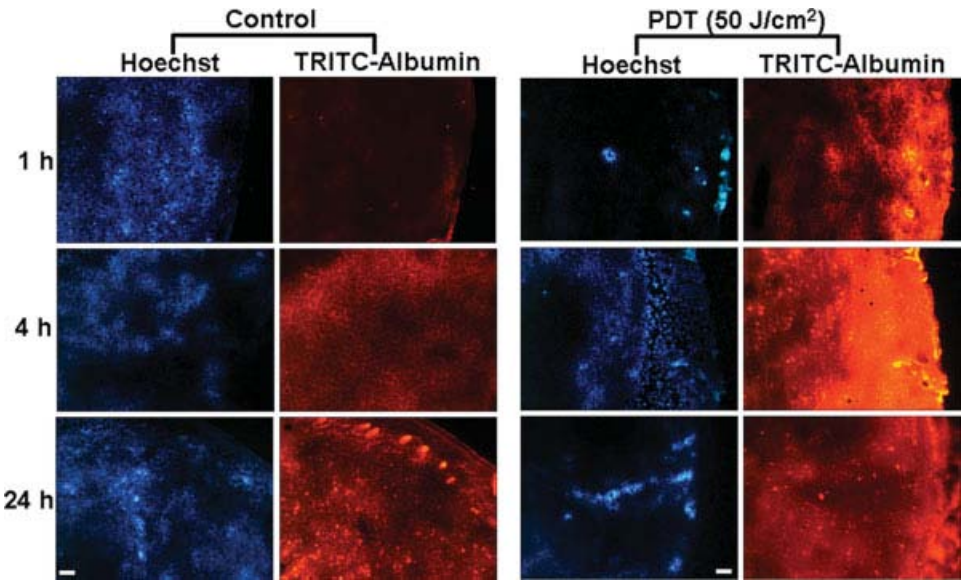

FIGURE 4 – *Ex vivo* fluorescence microscopy images showing the distribution of TRITC-albumin in relation to the functional blood vessels highlighted by Hoechst dye staining. The EGFP-MatLyLu tumors were treated with 50 J/cm^2 light at 15 min after i.v. injection of 0.25 mg/kg dose of verteporfin. Control tumors received no treatment. Immediately after treatment, tumor-bearing animals were i.v. injected with 20 mg/kg TRITC-albumin. Animals were euthanized at 1, 4 or 24 hr after injection of the TRITC-albumin. Hoechst dye (20 mg/kg) was i.v. injected at 1 min before euthanizing the animal. Frozen tumor sections from tissue samples were first imaged for Hoechst fluorescence and the same fields were then imaged for TRITC-albumin fluorescence. All images shown include the tumor periphery. Bars = 100 μm. [Color figure can be viewed in the online issue, which is available at www.interscience.wiley.com.]

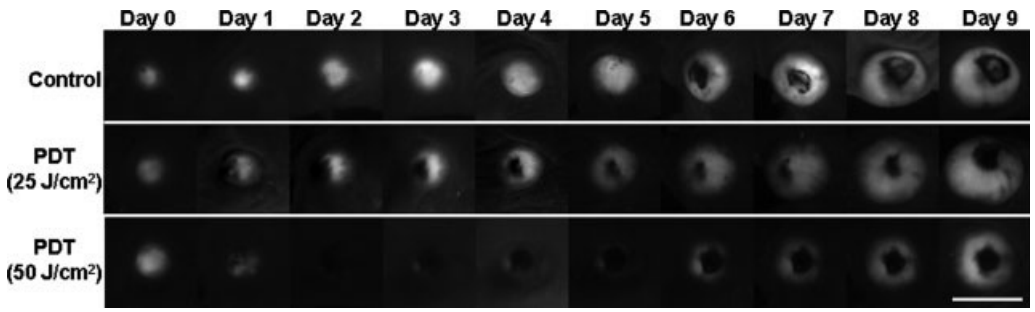

FIGURE 5 – *In vivo* tumor EGFP fluorescence images showing tumor response to vascular-targeting PDT with verteporfin. The EGFP-MatLyLu tumors were treated with 25 or 50 J/cm^2 light at 15 min after i.v. injection of 0.25 mg/kg dose of verteporfin. Tumor EGFP fluorescence was imaged daily for up to 9 days after treatment with a whole-body fluorescence imaging system as described in the Material and methods. Images at Day 0 were taken right before treatment. Control tumors received no treatment. Scale bar = 10 mm.

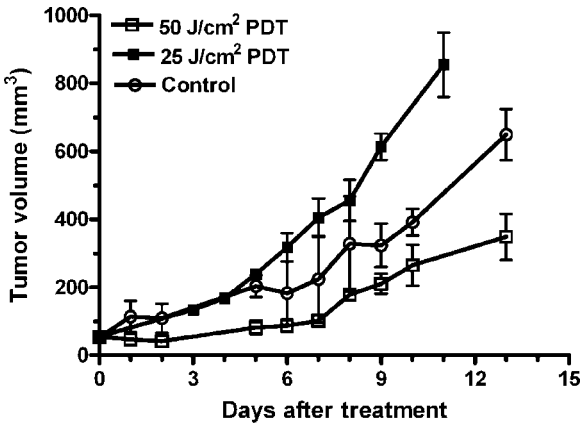

FIGURE 6 – Tumor volume changes after vascular-targeting PDT with verteporfin. The EGFP-MatLyLu tumors were treated with 25 or 50 J/cm^2 light at 15 min after i.v. injection of 0.25 mg/kg dose of verteporfin. Control tumors received no treatment. Tumor volume at Day 0 represented the starting volume right before the treatment.

blood vessels were mainly detected at the tumor periphery after PDT. In agreement with the macroscopic *in vivo* tumor imaging results, fluorescence microscopy also demonstrated a significant increase in the TRITC fluorescence intensity after PDT, especially in the tumor periphery.

Tumor response to vascular-targeting PDT was monitored noninvasively by whole body fluorescence imaging. The EGFP-MatLyLu tumors were imaged for EGFP fluorescence before and after treatments. Representative tumor EGFP fluorescence images are shown in Figure 5. Control tumors grew rapidly and exhibited central necrosis when tumor reached about 8–10 mm in diameter. Dead EGFP-MatLyLu tumor cells were unable to produce EGFP, causing dead tumor tissues to appear as dark areas in the EGFP fluorescence images. PDT with 25 J/cm^2 light dose induced a partial tumor necrosis, but this PDT condition failed to inhibit tumor growth (Fig. 5). In fact, tumor growth after this PDT treatment was even more rapid than control tumors and average tumor volume was nearly twice that of control tumors at 9 days after treatment (Fig. 6, $p < 0.01$). In contrast, the 50 J/cm^2 PDT effectively inhibited prostate tumor growth as indicated by a substantial decrease in EGFP fluorescence (Fig. 5) and average tumor volume (Fig. 6, $p < 0.01$ compared to the control tumor) after treatment. EGFP fluorescence was barely detectable at 2 days after PDT. But small EGFP fluorescent spots, indicating the existence of viable tumor cells, were often found at tumor edges several days after treatment and gradually grew in size which led to tumor recurrence. As shown in Figure 7, some viable tumor cells were clearly detected in tumor periphery at 48 hr after 50 J/cm^2 PDT.

Discussion

A whole-body animal fluorescence imaging system was used in this study to visualize noninvasively tumor response following PDT targeting of tumor blood vessels in an EGFP-expressing MatLyLu prostate tumor model. TRITC-albumin was used as a macromolecular probe to image tumor vascular barrier function (vascular permeability). The increase in the TRITC fluorescence intensity, caused by enhanced extravasation from blood vessels, is an indicator of vascular barrier disruption. Albumin has a plasma half-life of more than 24 hr and it was used to follow vascular permeability changes up to several hours after treatment.[22]

We found in the present study that vascular-targeting PDT increased vascular permeability in a dose-dependent manner, which is in agreement with our previous study and indicates that tumor vasculature is a primary target of PDT with verteporfin.[6] Importantly, our results demonstrate that the enhanced TRITC-albumin tumor uptake as a result of PDT-induced permeability increase was not homogeneous in tumor tissues. Both *in vivo* and *ex vivo* tumor imaging studies indicate that increase in TRITC-albumin extravasation was significantly higher in the peripheral tumor area than in the interior tumor area. Because the accumulation of a circulating molecule in tumor tissues is dependent upon the existence of functional blood vessels, the enhancement of TRITC-albumin accumulation in the tumor periphery is likely related to the predominant localization of functional blood vessels in peripheral tumor areas after vascular-targeting PDT. As shown in Figure 4, PDT was remarkably effective in inducing interior tumor blood vessel shutdown while some peripheral vessels were still functional up to 24 hr after PDT. Early closure of central tumor vessels limited the enhancement of TRITC-albumin in the tumor interior, whereas prolonged perfusion of some peripheral tumor vessels allowed more TRITC-albumin to continuously extravasate in the tumor periphery. We and others have previously reported that peripheral tumor vessels tend to maintain perfusion function after vascular-targeting PDT.[23–25] Our present results further demonstrate that continuous functioning of peripheral blood vessels, which had been permeabilized by PDT, led to preferential accumulation of circulating molecules in the tumor periphery.

The existence of functional blood vessels in the tumor periphery was associated with peripheral tumor cell survival after PDT. As shown in Figure 7, H&E staining indicated a rim of viable tumor cells in the tumor periphery at 48 hr after PDT in spite of extensive tumor necrosis. *In vivo* imaging of tumor EGFP fluorescence demonstrated that the survival of these peripheral tumor cells resulted in peripheral tumor recurrence (Fig. 5). Here we used EGFP as an indicator of tumor cell viability with the assumption that dead tumor cells are not able to synthesize EGFP and emit EGFP fluorescence. However, because EGFP has a half-life of more than 3 hr,[26] monitoring EGFP fluorescence shortly after treatment might not accurately report tumor cell viability. Sufficient time is needed for the degradation of EGFP synthesized

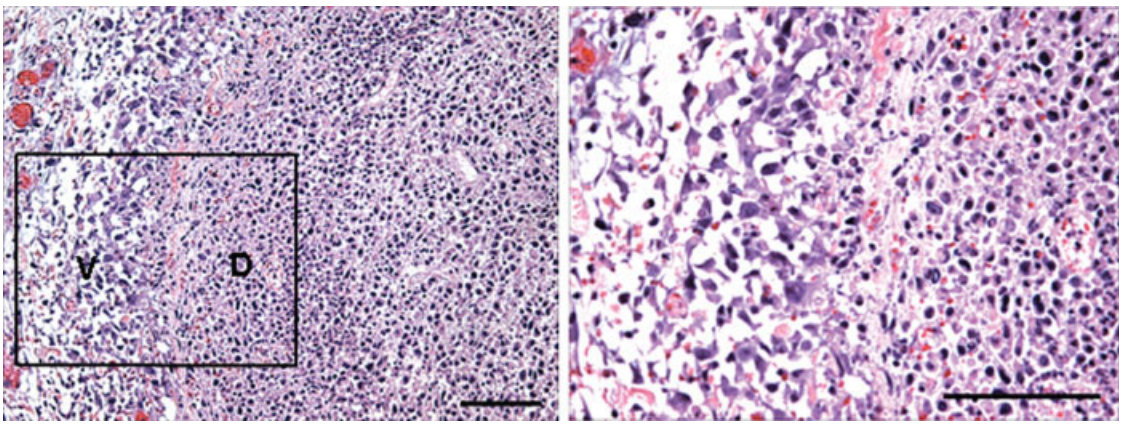

FIGURE 7 – H&E staining images showing the existence of viable tumor cells at the tumor periphery after vascular-targeting PDT with verteporfin. The EGFP-MatLyLu tumors were treated with 50 J/cm^2 light at 15 min after i.v. injection of 0.25 mg/kg dose of verteporfin. H&E staining of tumor sections taken at 48 hr after treatment showed wide spread tumor cell death and vascular damage. But a small number of viable tumor cells were detected at the tumor periphery. Part of the image on the left, highlighted in the box, is shown at a higher magnification on the right. The letters V and D indicate the viable tumor area and the dead tumor area, respectively. Bars = 100 μm. [Color figure can be viewed in the online issue, which is available at www.interscience.wiley.com.]

before treatment in order to use EGFP fluorescence to report cell viability. The observed decrease in EGFP fluorescence shortly after PDT in the present study was likely due to the oxidative degradation of EGFP during PDT rather than a real decrease in tumor cell viability. This was supported by the fact that there was little further decrease in EGFP fluorescence intensity over the following 5 hr period after PDT (Fig. 2*c*).

It is still not clear why peripheral tumor blood vessels react differently from interior blood vessels to vascular-targeting PDT. Understanding the mechanism behind this disparity in vascular response will help find ways to enhance the therapeutic effects of vascular-targeting PDT. Differences in vascular structure and function between tumor peripheral and interior blood vessels caused by morbid tumor pathobiology possibly contribute to such variations in vascular response. It is known that tumor tissues have higher tissue interstitial pressure than normal tissues because of leaky tumor blood vessels and poor lymphatic system function.[27,28] High tumor interstitial pressure is able to compress tumor vessels and lead to vessel collapse. Vessel compression and collapse are more severe in the tumor interior where tumor interstitial pressure is higher.[29,30] PDT has been shown to further increase tumor interstitial pressure as a result of enhancing vascular permeability.[31,32] Such an increase in tumor interstitial pressure will likely impose a greater compression on tumor blood vessels and cause vascular shutdown, especially in tumor interior areas. Moreover, we recently found that, compared to the interior tumor vessels, peripheral tumor blood vessels were generally larger and exhibited vascular lumen as well as more coverage of vascular pericytes and basement membrane.[33] Less mechanic compression together with more vessel supporting structures might make peripheral tumor vessels more resistant than the interior vessels to vessel closure induced by vascular-targeting PDT.

The survival of peripheral tumor cells as a consequence of disparity in vascular response between peripheral and interior blood vessels represents a therapeutic challenge for the vascular-targeting PDT. Several strategies can be adopted to eliminate or at least minimize surviving tumor cells at the tumor periphery. First of all, we could increase the PDT dose to determine whether a higher dose of vascular-targeting PDT will lead to the shutdown of both interior and peripheral tumor blood vessels, resulting in an increased tumor cure. Secondly, as combination therapies have been routinely used in cancer treatments, one approach of enhancing photodynamic vascular targeting effectiveness is to combine it with other cancer therapies. Combination therapies can be designed based on different targeting principles. Targeting both tumor vascular and cellular compartments by combining vascular-targeting PDT with a cancer cell-targeted therapy could be a promising strategy because the increased vascular permeability induced by PDT has been shown to enhance drug delivery.[6,34,35] Our present study further demonstrates that the enhancement of drug accumulation mainly occurred at the tumor periphery where tumor cell survival tends to occur after vascular-targeting PDT. Therefore, combining vascular-targeting PDT with other anticancer drug therapies will allow more anticancer agents to be preferentially deposited in the peripheral tumor area to kill tumor cells that otherwise might survive after PDT treatment.

In summary, we utilized *in vivo* animal fluorescence imaging combined with standard *ex vivo* tissue fluorescence microscopy to examine changes in vascular function and tumor cell viability after vascular-targeting PDT. Our results indicate that, although PDT causes an overall increase in vascular permeability, peripheral tumor blood vessels are somehow able to maintain perfusion function whereas interior blood vessels are shutdown shortly after PDT. Such a disparity in vascular response is conducive to peripheral tumor cell survival and also explains the preferential accumulation of circulating molecules in the tumor periphery. We are currently investigating the mechanisms underlying this response disparity and exploring therapeutic strategies that minimize the survival of peripheral tumor cells.

Acknowledgements

The authors gratefully acknowledge Dr. Tayyaba Hasan of the Wellman Center for Photomedicine for helpful discussions and QLT Inc. for providing verteporfin.

References

1. Dougherty TJ, Gomer CJ, Henderson BW, Jori G, Kessel D, Korbelik M, Moan J, Peng Q. Photodynamic therapy. J Natl Canc Inst 1998; 90:889–905.
2. Schmidt R. Photosensitized generation of singlet oxygen. Photochem Photobiol 2006;82:1161–77.
3. Chen B, Pogue BW, Hoopes PJ, Hasan T. Vascular and cellular targeting for photodynamic therapy. Crit Rev Eukaryot Gene Expr 2006;16:279–305.
4. Brown SB, Mellish KJ. Verteporfin: a milestone in opthalmology and photodynamic therapy. Expert Opin Pharmacother 2001;2:351–61.

5. Chen B, Pogue BW, Hoopes PJ, Hasan T. Combining vascular and cellular targeting regimens enhances the efficacy of photodynamic therapy. Int J Radiat Oncol Biol Phys 2005;61:1216–26.
6. Chen B, Pogue BW, Luna JM, Hardman RL, Hoopes PJ, Hasan T. Tumor vascular permeabilization by vascular-targeting photosensitization: effects, mechanism, and therapeutic implications. Clin Canc Res 2006;12:917–23.
7. Liu DL, Svanberg K, Wang I, Andersson-Engels S, Svanberg S. Laser Doppler perfusion imaging: new technique for determination of perfusion and reperfusion of splanchnic organs and tumor tissue. Laser Surg Med 1997;20:473–9.
8. Enejder AM, af Klinteberg C, Wang I, Andersson-Engels S, Bendsoe N, Svanberg S, Svanberg K. Blood perfusion studies on basal cell carcinomas in conjunction with photodynamic therapy and cryotherapy employing laser-Doppler perfusion imaging. Acta Derm Venereol 2000;80:19–23.
9. Yu G, Durduran T, Zhou C, Wang HW, Putt ME, Saunders HM, Sehgal CM, Glatstein E, Yodh AG, Busch TM. Noninvasive monitoring of murine tumor blood flow during and after photodynamic therapy provides early assessment of therapeutic efficacy. Clin Canc Res 2005;11:3543–52.
10. Kruijt B, de Bruijn HS, van der Ploeg-van den Heuvel A, Sterenborg HJ, Robinson DJ. Laser speckle imaging of dynamic changes in flow during photodynamic therapy. Laser Med Sci 2006;21:208–12.
11. Smith TK, Choi B, Ramirez-San-Juan JC, Nelson JS, Osann K, Kelly KM. Microvascular blood flow dynamics associated with photodynamic therapy, pulsed dye laser irradiation and combined regimens. Laser Surg Med 2006;38:532–9.
12. Aalders MC, Triesscheijn M, Ruevekamp M, de Bruin M, Baas P, Faber DJ, Stewart FA. Doppler optical coherence tomography to monitor the effect of photodynamic therapy on tissue morphology and perfusion. J Biomed Opt 2006;11:044011.
13. Ohlerth S, Laluhova D, Buchholz J, Roos M, Walt H, Kaser-Hotz B. Changes in vascularity and blood volume as a result of photodynamic therapy can be assessed with power Doppler ultrasonography. Laser Surg Med 2006;38:229–34.
14. Schmidt-Erfurth U, Niemeyer M, Geitzenauer W, Michels S. Time course and morphology of vascular effects associated with photodynamic therapy. Ophthalmology 2005;112:2061–9.
15. Zilberstein J, Schreiber S, Bloemers MC, Bendel P, Neeman M, Schechtman E, Kohen F, Scherz A, Salomon Y. Antivascular treatment of solid melanoma tumors with bacteriochlorophyll-serine-based photodynamic therapy. Photochem Photobiol 2001;73:257–66.
16. Seshadri M, Spernyak JA, Mazurchuk R, Camacho SH, Oseroff AR, Cheney RT, Bellnier DA. Tumor vascular response to photodynamic therapy and the antivascular agent 5,6-dimethylxanthenone-4-acetic acid: implications for combination therapy. Clin Canc Res 2005; 11:4241–50.
17. Yang M, Baranov E, Jiang P, Sun FX, Li XM, Li L, Hasegawa S, Bouvet M, Al-Tuwaijri M, Chishima T, Shimada H, Moossa AR, et al. Whole-body optical imaging of green fluorescent protein-expressing tumors and metastases. Proc Natl Acad Sci USA 2000;97:1206–11.
18. Hoffman RM. The multiple uses of fluorescent proteins to visualize cancer in vivo. Nat Rev Canc 2005;5:796–806.
19. Ntziachristos V. Fluorescence molecular imaging. Annu Rev Biomed Eng 2006;8:1–33.
20. Nguyen TH, Oberholzer J, Birraux J, Majno P, Morel P, Trono D. Highly efficient lentiviral vector-mediated transduction of nondividing, fully reimplantable primary hepatocytes. Mol Ther 2002;6:199–209.
21. Pogue BW, Gibbs SL, Chen B, Savellano M. Fluorescence imaging in vivo: raster scanned point-source imaging provides more accurate quantification than broad beam geometries. Technol Canc Res Treat 2004;3:15–21.
22. Matsushita S, Chuang VT, Kanazawa M, Tanase S, Kawai K, Maruyama T, Suenaga A, Otagiri M. Recombinant human serum albumin dimer has high blood circulation activity and low vascular permeability in comparison with native human serum albumin. Pharm Res 2006;23:882–91.
23. Chen B, Pogue BW, Goodwin IA, O'Hara JA, Wilmot CM, Hutchins JE, Hoopes PJ, Hasan T. Blood flow dynamics after photodynamic therapy with verteporfin in the RIF-1 tumor. Radiat Res 2003; 160:452–9.
24. Kurohane K, Tominaga A, Sato K, North JR, Namba Y, Oku N. Photodynamic therapy targeted to tumor-induced angiogenic vessels. Cancer Lett 2001;167:49–56.
25. Koudinova NV, Pinthus JH, Brandis A, Brenner O, Bendel P, Ramon J, Eshhar Z, Scherz A, Salomon Y. Photodynamic therapy with Pd-bacteriopheophorbide (TOOKAD): successful in vivo treatment of human prostatic small cell carcinoma xenografts. Int J Canc 2003; 104:782–9.
26. Li X, Zhao X, Fang Y, Jiang X, Duong T, Fan C, Huang CC, Kain SR. Generation of destabilized green fluorescent protein as a transcription reporter. J Biol Chem 1998;273:34970–5.
27. Fukumura D, Jain RK. Tumor microenvironment abnormalities: causes, consequences, and strategies to normalize. J Cell Biochem 2007;101:937–49.
28. Heldin CH, Rubin K, Pietras K, Ostman A. High interstitial fluid pressure - an obstacle in cancer therapy. Nat Rev Canc 2004;4:806–13.
29. Rofstad EK, Tunheim SH, Mathiesen B, Graff BA, Halsor EF, Nilsen K, Galappathi K. Pulmonary and lymph node metastasis is associated with primary tumor interstitial fluid pressure in human melanoma xenografts. Canc Res 2002;62:661–4.
30. Boucher Y, Jain RK. Microvascular pressure is the principal driving force for interstitial hypertension in solid tumors: implications for vascular collapse. Canc Res 1992;52:5110–14.
31. Fingar VH, Wieman TJ, Doak KW. Changes in tumor interstitial pressure induced by photodynamic therapy. Photochem Photobiol 1991; 53:763–8.
32. Leunig M, Goetz AE, Gamarra F, Zetterer G, Messmer K, Jain RK. Photodynamic therapy-induced alterations in interstitial fluid pressure, volume and water content of an amelanotic melanoma in the hamster. Br J Canc 1994;69:101–3.
33. Chen B, He C, de Witte P, Hoopes PJ, Hasan T, Pogue BW. Vascular targeting in photodynamic therapy. In: Hamblin MR, Mroz P, eds. Advances in photodynamic therapy: basic, translational and clinicaled. Norwood, MA: Artech House Inc (in press).
34. Snyder JW, Greco WR, Bellnier DA, Vaughan L, Henderson BW. Photodynamic therapy: a means to enhanced drug delivery to tumors. Canc Res 2003;63:8126–31.
35. Debefve E, Pegaz B, Ballini JP, Konan YN, van den Bergh H. Combination therapy using aspirin-enhanced photodynamic selective drug delivery. Vascul Pharmacol 2007;46:171–80.

CHAPTER 9

Vascular Targeting in Photodynamic Therapy

Bin Chen, Chong He, Peter de Witte, P. Jack Hoopes, Tayyaba Hasan, and Brian W. Pogue

9.1 Introduction

The mechanism of PDT in cancer treatment is complicated and evolves as our understanding of cancer biology and pharmacology progresses. It is now clear that PDT can either directly kill tumor cells or indirectly induce tumor cell death as a result of direct damage to tumor stroma [1]. Adequate and simultaneous deposition of a photosensitizer, light, and oxygen molecules in tumor cells will cause tumor cell death. However, this direct photocytotoxicity is often limited (generally less than 1-log) in tumor cell killing likely due to inadequate supply of photosensitizers, light, and/or oxygen in tumor tissues [2]. Tumor vasculature is an important target of PDT and this indirect tumor targeting mechanism is mainly responsible for the acute decrease of tumor burden after PDT with most photosensitizers [1]. Furthermore, PDT-induced inflammation as well as direct photosensitizing effects on immune cells may activate the body immune system and lead to the generation of tumor-specific immunity, which is important for maintaining long-term tumor control [3].

For most photosensitizers, vascular damage is the predominant PDT effect and primarily responsible for the final treatment outcome [1]. Because of this, vascular-targeting PDT has been developed to further potentiate vascular damage. In this chapter, we will focus on vascular targeting in PDT. This targeting mechanism has led to so far the most successful application of PDT and is showing great promise in cancer treatment as well. We will discuss photodynamic vascular targeting principle, mechanisms, challenges, and strategies to enhance its therapeutic outcome.

9.2 Tumor Vascular Targeting

It is well-known that solid tumors cannot grow larger than about 1 mm^3 without developing a vascular network [4]. This is because, similar to normal tissues, tumor tissues require a functional vascular system for the delivery of nutrients and the removal of metabolic waste. To sustain tumor growth, tumor tissues need to depend upon existing host vessels as well as develop new blood vessels for blood supply. Compared to the normal vasculature, tumor blood vessels exhibit significant abnor-

malities in vessel architecture (e.g., tortuousity, dilatation, irregular branching, and lack of pericyte and basement membrane coverage) and function (e.g., stagnant blood flow, increased vascular permeability) [5]. Although the mechanisms leading to tumor vessel structural and functional abnormalities are not well understood, the imbalance between pro- and antiangiogenic factors and mechanical compression generated by high tumor interstitial pressure and proliferating tumor cells have been suggested to be the major contributing factors [5]. The differences between tumor versus normal vasculature in the vessel molecular signature, structure, and function provide the basis for selective tumor vascular targeting.

Vascular targeting therapy can be divided into antiangiogenic therapy that inhibits the formation of new vessels and vascular disrupting therapy that targets the existing blood vessels [6]. The overall goal of tumor vascular targeting therapy is to selectively disrupt or modulate tumor vascular function for the therapeutic purposes without affecting much normal tissue functions. This modality can be used alone as monotherapy, but more often it is used in combination with other therapies in cancer treatment. Tumor vascular targeting strategy has several apparent advantages over the conventional tumor cellular targeting approach [4, 7]. First, vascular targets are readily accessible to the therapeutic agents delivered intravenously whereas tumor cellular targets are typically difficult to reach due to the existence of various physiological barriers. Second, vascular targeting is highly efficient and potent in tumor cell killing because, unlike tumor cell-targeted therapies, not all the endothelial cells are necessary to be targeted to disrupt tumor vascular function. Instead, damage to a single endothelial cell or a portion of blood vessel may induce catastrophic effect on tumor perfusion, resulting in killing thousands of tumor cells that are dependent upon that vessel for blood supply. Third, because endothelial cells are generally considered to be more genetically stable than tumor cells, the risk of acquiring drug resistance is usually low. These advantages render tumor vascular targeting a promising approach in current cancer therapy.

9.3 Principle of Photodynamic Vascular Targeting

Photodynamic vascular targeting is based on site-directed delivery of photosensitizing agents to the vascular system followed by light irradiation to induce site-specific vascular photosensitizing effects. Since vasculature-directed photosensitizer delivery can be achieved by passive or active means, photodynamic vascular targeting can be further divided into passive or active targeting approach [1]. The passive vasculature-directed photosensitizer delivery is primarily based on the innate photosensitizer pharmacokinetic property that plasma drug level is often high shortly after intravenous administration of a photosensitizer (Color Plate 4). As can be seen, fluorescence image of hypericin (a) and the corresponding H&E staining photograph (b) demonstrate the intravascular localization of hypericin at 30 minutes after i.v. injection of a 5-mg/kg dose of hypericin in the RIF-1 mouse tumor model. Vascular-targeting PDT with hypericin, (i.e., light treatment at 30 minutes after a 5-mg/kg dose of hypericin injection, caused vascular shutdown in central tumor areas). However, some tumor peripheral blood vessels were still functional, as indicated by the presence of Hoechst dye fluorescence (c), which was injected 1

minute before euthanizing the animal. The corresponding H&E staining image (d) confirmed the vessel histology. Vascular-targeting PDT with hypericin (i.e., light treatment at 30 minutes after a 1-mg/kg dose of hypericin injection), significantly inhibited the RIF tumor growth and its antitumor effect was further enhanced by subcutaneous injection of antiangiogenic drug TNP-470 at a dose of 30 mg/kg once every 2 days. Each group included 8 to 10 animals (Figure 9.1).

This time period when photosensitizer is mainly localized inside the vasculature provides a temporal window for the passive vascular targeting. Although the exact location of this temporal window is largely dependent on the plasma kinetics of individual photosensitizer, for most photosensitizers it typically occurs within 60 minutes after injection.

By contrast, active vascular-targeting PDT seeks to achieve vasculature-directed drug delivery by altering photosensitizer pharmacokinetic property through drug structure modification or drug formulation into a targeted delivery system [1]. A targeting moiety that has a high affinity to endothelial cell markers (e.g., integrins, VEGF receptors, tumor endothelial markers) or vessel supporting structures (e.g., fibronectin with ED-B domain) is often used in the photosensitizer modification. The resulting photosensitizer conjugates are expected to be selectively accumulated in the targeted blood vessels, leading to a site-specific photosensitization upon light activation.

9.4 Mechanisms of Photodynamic Vascular Targeting

Photodynamic vascular targeting therapy has been shown to produce reactive oxygen species intravascularly, in particular singlet oxygen, which is believed to be mainly responsible for the subsequent vessel structural and functional alterations [8]. The ultimate goal of vascular-targeting PDT in cancer therapy is to obtain maximal tumor cell killing by inducing tumor vascular shutdown. The mechanism of

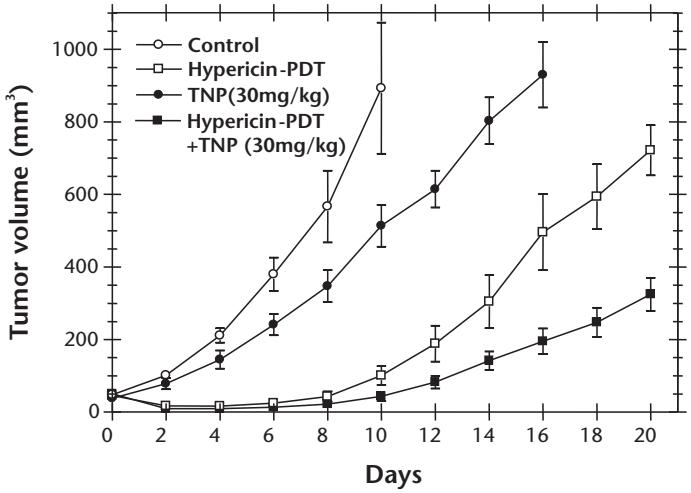

Figure 9.1 Tumor inhibition after vascular-targeting PDT with hypericin and antiangiogenic drug TNP-470.

PDT-induced vascular shutdown is complicated because it likely involves multiple targets in the blood cells and blood vessels, which are interweaved in complex cascades of events. Intravital fluorescence microscopic study demonstrates that microcirculation dysfunction after vascular-targeting PDT is induced by at least two vascular events, vessel occlusion induced by thrombus formation and vessel constriction/collapse caused by mechanic compression and vasoactive substances (Figure 9.2(a) and (b)).

Thrombus formation can be induced by photosensitizing damage to either blood cells or endothelial cells. It has been shown that PDT can cause platelet aggregation and thrombus formation by direct damage to the platelet and red blood cell membranes [9, 10]. Damage to the platelets may further stimulate the release of thromboxane, a vasoactive substance with potent vessel constriction and thrombus formation effects [11]. More often, PDT-induced damage to the blood cells is coupled with damage to the endothelial cells, which might explain why blood cell aggregation is often observed starting from the vessel wall. Since endothelium serves as an interface between blood and underneath tissue, loss of endothelial barrier as a result of vascular photosensitization exposes tissue extracellular matrix to the circulation, which activates platelets and polymorphonuclear leukocytes and induces blood cell adherence to the damaged endothelial cells. Thromboxane release as a result of platelet activation has been shown to contribute significantly to vessel constriction and thrombus formation, which can be inhibited by thromboxane inhibitors aspirin and indomethacin [12] or platelet depletion [11]. Endothelial cells also

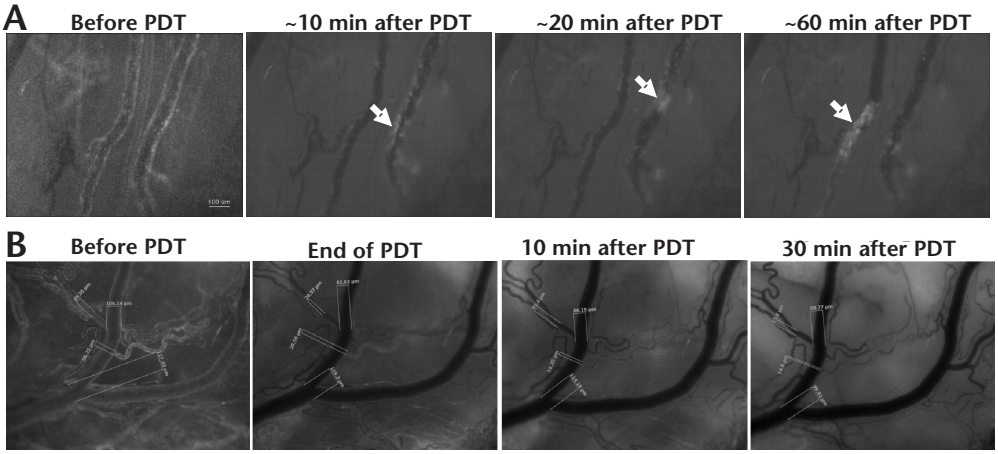

Figure 9.2 (a) Intravital fluorescence microscopic images showing intravascular localization of verteporfin and thrombus formation after vascular-targeting PDT in the orthotopic MatLyLu rat prostate tumor. Rat blood cells were labeled with fluorescent dye DiI and injected (i.v.) into the animals to highlight blood vessels. The MatLyLu tumors were treated with 50-J/cm^2 light (690 nm, at 50 mW/cm^2) at 15 minutes after i.v. injection of 0.25-mg/kg verteporfin to target tumor blood vessels. Blood cell adherence and thrombus formation, indicated by arrows, were clearly visible after vascular-targeting PDT. (b) Intravital fluorescence microscopic imaging of vascular permeability increase and vessel compression after vascular-targeting PDT with verteporfin. Animals were i.v. injected with 10-mg/kg 2,000-kDa FITC-dextran right before irradiation and imaged every 2 minutes for the FITC fluorescence during and after PDT. The images shown are right before PDT, immediately, 10 minutes, and 30 minutes after PDT. Sizes of some blood vessels are labeled on the images.

influence blood clotting balance by releasing von Willebrand factor that facilitates thrombus formation [13] and prostacyclin that inhibits thrombus formation and dilates blood vessels [14]. The net effect likely favors clot formation at least at early stage after vascular photosensitization. Blood clots formed inside vessel lumen cause obstruction to blood flow. However, blood vessels may resume perfusion because not all the clots are stable and some of them can be dissolved and dislodged possibly by body anticoagulants. Only the stable thrombi will finally occlude blood vessels and shut down vascular function. Inhibition of thrombus formation by heparin has been shown to delay PDT-induced blood flow stasis [15]. But it is not able to completely inhibit blood flow decrease, suggesting that thrombus formation is only partially responsible for the vascular damage induced by PDT.

As a spontaneous response to blood vessel damages, vessel constriction is often observed after vascular photosensitization, which also contributes to PDT-induced blood flow stasis (Figure 9.3).

Vessel constriction can be caused by the release of vasoactive substances such as thromboxane and leukotrienes [16]. However, a strong inducer of vessel constriction and even collapse in tumor tissues comes from the increase of interstitial fluid pressure [5]. It is well-established that tumor tissues generally have higher tissue interstitial pressure than the normal tissues because of leaky tumor blood vessels. The mechanic compression generated by high tumor interstitial pressure can collapse tumor blood vessel even without treatment and this is one of the mechanisms involved in acute hypoxia development in tumor tissues [17]. Such vessel compression/collapse effects are aggravated by PDT because PDT is able to cause vascular barrier disruption and therefore further increase tumor interstitial pressure [18, 19].

Since endothelial cells play a critical role in maintaining vascular barrier and perfusion functions, it is important to study how endothelial cells respond to photosensitization at cellular and molecular levels. Studies with different photosensitizers have shown that photosensitization of endothelial cells induces rapid microtubule

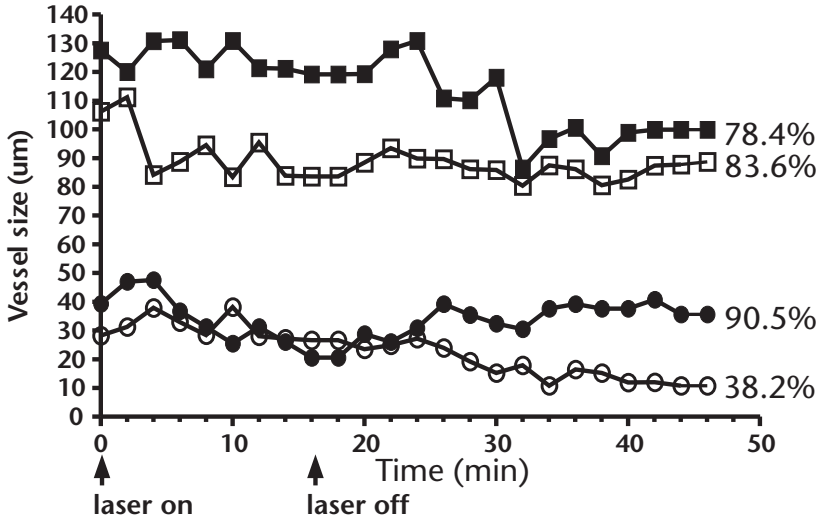

Figure 9.3 The change of blood vessel size during and after vascular-targeting PDT with verteporfin. Sizes of four blood vessels shown in Figure 9.2b were measured and the percentages over pretreatment sizes are shown.

depolymerization followed by stress fiber actin formation and cell rounding [20, 21].

Although it is not clear how microtubule damage results in endothelial cell shape change, microtubule depolymerization is believed to initiate subsequent vessel functional changes because endothelial cell barrier function is dependent on endothelial cell morphology regulated by cell cytoskeleton. Indeed, photosensitization-induced endothelial cell shape change has been shown to be correlated to the permeability increase [21]. Increase in cytosol calcium concentration has been suggested to be the cause of microtubule depolymerization [20]. However, direct photosensitizing damage to the microtubules cannot be ruled out. Vascular permeability increase has been observed in both animal and human studies shortly after PDT [16, 22], suggesting that this is an early event following endothelial cell damage (Figure 9.4).

The disruption of vascular barrier function will trigger the subsequent thrombus formation and vessel compression as described above.

The molecular mechanism involved in endothelial photosensitization is poorly studied. There are reports showing that photosensitization activates nuclear transcriptor NF-κB in endothelial cells through a reactive oxygen species-mediated mechanism [23, 24]. Since NF-κB is major regulator of inflammatory and immune reactions, its activation in endothelial cells plays an important role in vascular photosensitization-induced tumor destruction. Paradoxically, NF-κB activation can cause both tumor inhibition and stimulation [25]. Tumor inhibition is related to its role in enhancing gene expression of cytokines (IL-6, TNF-α), adhesion molecules (intercellular adhesion molecule-1, vascular cell adhesion molecule-1), and possibly heat shock proteins [24, 26]. As a result, vascular photosensitization treatment is able to stimulate blood cells, especially neutrophils adhesion to the endothelial cells, inducing vascular damages. On the other hand, tumor stimulation as a consequence of NF-κB activation is associated with the upregulation of cyclooxygenas-2 (COX-2), matrix metalloproteases (MMPs), and inhibitors of apoptosis [25]. Although there is no report demonstrating the upregulation of COX-2 and

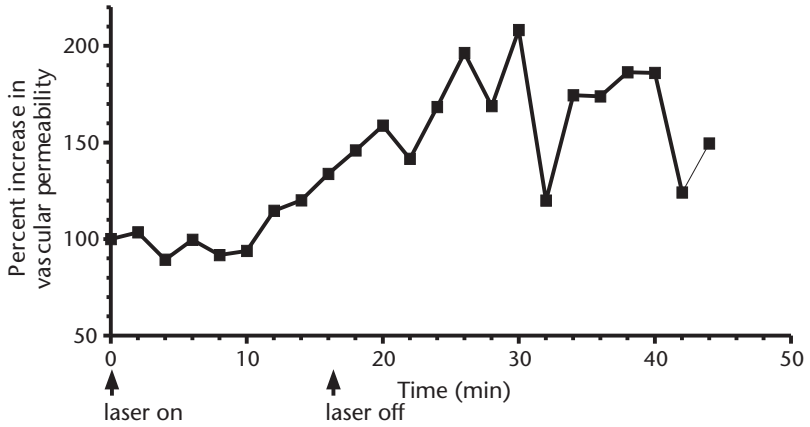

Figure 9.4 The change of vascular permeability during and after vascular-targeting PDT with verteporfin. Vascular permeability change was determined by measuring the 2,000-kDa FITC-dextran fluorescence intensity from the above intravital microscopic images Figure 9.2b, and normalizing the aftertreatment intensity values to the pretreatment value.

apoptosis inhibitors in endothelial cells, which has been shown in tumor cells, the induction of MMP-9 expression has been confirmed in endothelial cells after PDT, suggesting a role of NF-κB activation in endothelial resistance to photosensitization [25]. Interestingly, pretreatment of endothelial cells with PDT or other oxidative stress inducers has been shown to induce cell adaptation, resulting in the upregulation of heat shock protein and antioxidation enzymes through the p38 MARK pathway. This cellular adaptation to the oxidative stressors indeed renders endothelial cells' resistance to the subsequent treatment [27].

9.5 Therapeutic Challenges of Photodynamic Vascular Targeting

Although vascular-targeting PDT is able to induce extensive tumor vascular shutdown, and consequently, tumor cell death, functional blood vessels are typically detected at tumor peripheral areas following noncurative treatments. The existence of these functional blood vessels can lead to tumor recurrence, which is often observed starting from the peripheral tumor area [28, 29]. Figure 9.5 shows representative tumor fluorescence images after verteporfin-PDT.

In this experiment, we used a lentivirus-transduced MatLyLu prostate tumor cell line that permanently expresses EGFP. The EGFP-MatLyLu tumors were imaged noninvasively for the EGFP fluorescence before and after PDT by using a whole-body fluorescence imaging system. Because dead EGFP-MatLyLu tumor cells were not able to produce EGFP, dead tumor tissues would appear as dark areas and only viable tumor tissues could be visible on tumor EGFP fluorescence images. Control tumors grew rapidly and generally exhibited central necrosis when a tumor reached about 8 to 10 mm in diameter. The 50-J/cm^2 PDT was effective in eradicating tumor tissue and little EGFP fluorescence was detected by 2 days after PDT. However, small EGFP fluorescent spots, indicating the existence of viable tumor cells, were detected at tumor edges several days after treatment. Peripheral viable tumor tissues were found growing rapidly, leading to tumor recurrence.

It is still not clear why tumor peripheral and central blood vessels react differently to the vascular photosensitization. It is hypothesized that such a variation in vascular response is likely related to the differences in tumor interstitial pressure and the structure of blood vessels in tumor central versus peripheral areas. Because

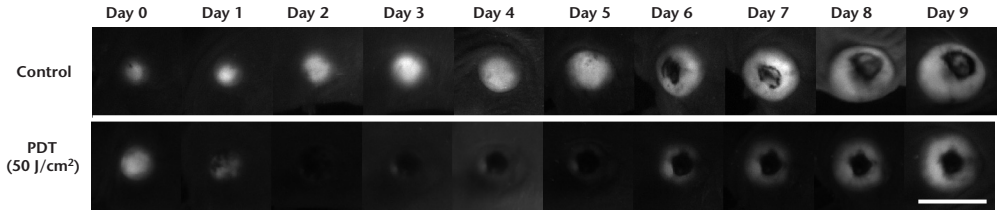

Figure 9.5 Noninvasive fluorescence imaging of tumor response after vascular-targeting PDT with verteporfin. The EGFP-MatLyLu tumors were imaged with a whole-body fluorescence imaging system before and after the vascular-targeting PDT, showing tumor recurrence starting from 3 days after treatment. Images of control tumor receiving no treatment are also shown for comparison. Bar=10 mm.

the tumor central area generally has a higher interstitial pressure than the peripheral area, central blood vessels are more likely to collapse than the peripheral vessels as a result of higher mechanic compression [30, 31]. Moreover, peripheral tumor blood vessels are generally found to be larger and have more vessel supporting structures such as pericytes than the central tumor vessels (Figure 9.6).

Collectively, less tumor interstitial pressure together with more vessel supporting structures might make peripheral tumor vessels more resistant to the vessel compression/collapse imposed by PDT-induced tumor interstitial pressure elevation. Survival of these peripheral blood vessels after vascular photosensitization provides a chance of survival to the tumor cells supported by these vessels.

To maintain tissue integrity and function, biological systems develop sets of well-balanced repairing and adaptive mechanisms to deal with various internal and external damages. Through complicated and often redundant signaling cascades, cells are able to survive nonfatal damages by stimulating cell growth, tissue angiogenesis, and remodeling. Unfortunately, tumor endothelial and tumor cells can hijack these spontaneous responses to obtain their own survival after subcurative treatments, leading to disease recurrence. As mentioned above, photosensitization activates p38 MAPK survival signaling in endothelial cells [27]. The activation of p38 MARK is able to further induce the upregulation of COX-2, which catalyzes the conversion of arachidonic acid to prostaglandins (PGs) [32, 33]. PGs, especially PGE2, have been shown to enhance cell motility, adhesion, and survival, and stimulate tumor angiogenesis by inducing VEGF release. Furthermore, elevated VEGF release can also be obtained via HIF-1-mediated signaling pathway activated by PDT-induced tissue hypoxia [34, 35]. Through the activation of these self-repairing and surviving pathways, tumor endothelial and tumor cells actually create a favorable microenvironment to maintain their survival and growth. It is not unusual to observe that tumor cells after subcurative PDT treatments are actually becoming

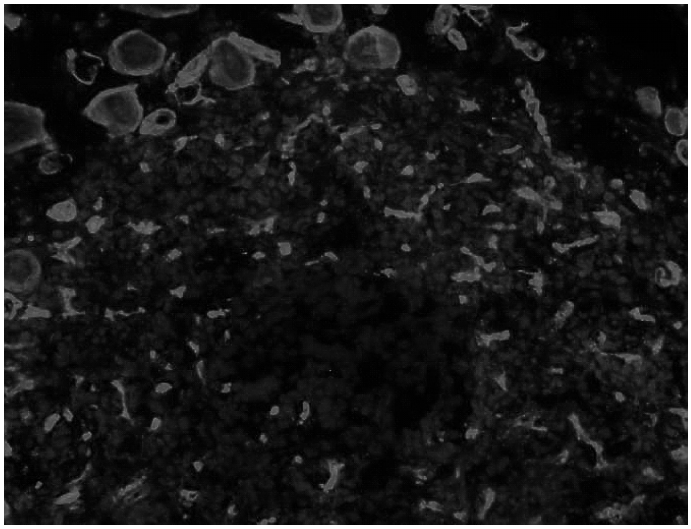

Figure 9.6 Immunohistochemical staining showing the difference in vessel morphology and structure between tumor peripheral and central blood vessels. Blood vessel pericyte marker α-small muscle actin (α-SMA) staining indicates that peripheral vessels are generally bigger and have better pericyte coverage than central vessels. Note the existence of central necrosis.

more aggressive [35, 36]. In the end, noncurative treatments might unintentionally select a small population of cells that are good at manipulating normal physiological pathways to survive therapeutic stressors. Therefore, how to target cell survival signals and adaptation mechanisms represents a major therapeutic challenge for not only photodynamic vascular targeting, but also all other cancer therapies.

9.6 Current Status of Photodynamic Vascular Targeting

Passive vascular-targeting PDT provides an effective way of targeting blood vessels and has been successfully translated into clinical application for diseases characterized by the overproliferation of blood vessels. Based on this mechanism, verteporfin is currently being used for the treatment of age-related macular degeneration (AMD) and more photosensitizers such as tin ethyletiopurpurin (SnET2, Purlytin) and lutetium texaphyrin (Lu-Tex, Optrin) are under clinical trials for AMD. Quite a few photosensitizers have also been evaluated for cancer treatment based on this passive targeting mechanism [1]. Among these photosensitizes, Tookad is at the forefront in the development pipeline. Currently, Tookad is in a phase I/II clinical trial for locally recurrent prostate cancer after radiation therapy [37]. Although limited in the number of studies, active vascular-targeting PDT is being pursued actively for the treatment of cancer and noncancer diseases. Promising results have been obtained from several studies of conjugating photosensitizers to the blood vessel-homing peptides [38–42].

9.7 Strategies to Enhance Photodynamic Vascular Targeting

As combination therapy has been routinely used in cancer treatment, one approach of enhancing photodynamic vascular targeting efficacy is to combine it with other cancer therapies. Combination therapies can be designed based on several different targeting principles. Targeting both tumor vascular and cellular compartments by combining photodynamic vascular targeting therapy with a cancer cell-targeted therapy has been demonstrated to be an effective strategy. For instance, more than additive antitumor effects have been obtained from most early studies exploring the combination of PDT and cancer chemotherapy [43, 44]. Recently, PDT itself has been studied for targeting tumor blood vessels or tumor cells, and enhanced therapeutic effects have been reported from studies with combined PDT regimens that target both tumor compartments. These dual targeting PDT treatments include PDT using a vascular-targeting photosensitizer Photofrin in combination with PDT using a cellular-targeting photosensitizer 5-aminolevulinic acid (5-ALA) [45], PDT regimen based on photosensitizer dose fractionation protocol so that light can be delivered when photosensitizer has been deposited in both vascular and cellular compartments [46], and sequential combination of a cancer cell-targeted PDT followed by a blood vessel-targeted PDT [28].

Although the mechanisms responsible for such enhanced antitumor effects are still not clear, spatial cooperation in tumor cell killing between vascular-targeting PDT and cancer cell-targeted therapies possibly plays a role here. As mentioned

above, vascular-targeting PDT is especially effective in inducing central tumor cell death. Cancer cell-targeted therapies however mainly kill peripheral PDT tumor cells because most anticancer agents, including photosensitizers, tend to accumulate more at the tumor periphery presumably because of better perfusion at tumor peripheral areas [47, 48]. Thus, cancer cell-targeted therapies may complement vascular-targeting PDT in reducing some peripheral tumor cells that are otherwise not able to be killed by vascular-targeting PDT. The other mechanism possibly involved in the therapeutic enhancement is that both conventional and vascular-targeting PDT treatments have been shown to improve drug delivery to tumor tissues as a result of PDT-induced vascular permeability increase [21, 49]. Interestingly, we have found that such an enhancement in tumor drug delivery caused by vascular-targeting PDT is actually more pronounced in the tumor peripheral area than in the tumor central area (observation not yet published). The overall increase of the anticancer agent in the tumor tissue, tumor peripheral areas in particular, after vascular-targeting PDT may also account for the improved antitumor effect.

The other important combination strategy is to target the surviving and repairing pathways that tumor endothelial cells as well as tumor cells depend on to maintain their survival after vascular-targeting PDT. An example in this case is the combination of vascular-targeting PDT with antiangiogenic therapy. PDT treatments have been found to stimulate angiogenesis and tumor growth by inducing VEGF upregulation [34, 35]. Depending on the photosensitizer, the type of tumor model, and treatment conditions, the elevation of VEGF can be caused by hypoxia-induced HIF-1 activation [34], COX-2 overexpression [33, 50] and p38 MAPK activation [35]. Thus, combined treatments of PDT with VEGF antibody bevacizumab [51], antiangiogenic drug TNP-470 [52] or COX-2 inhibitor [50] have all been shown to enhance the therapeutic effects. As our understanding regarding tumor/endothelial cell adaptation to therapeutic stressors increases, more such rationale-designed combination regimens will be designed to target crucial cellular and molecular surviving pathways, leading to a synergistic treatment outcome.

9.8 Summary and Conclusions

Vascular damage is the most important mechanism involved in PDT-mediated tumor eradication. Vascular-targeting PDT is designed to further strengthen this vascular photosensitization effect by site-directed delivery of photosensitizing agents to the vascular targets. Being so far the most successful PDT regimen, vascular-targeting PDT has been used clinically in the management of AMD and is showing great promise in cancer treatment as well. However, spatial heterogeneity in the vascular response and tumor/endothelial cell adaptation to the oxidative and hypoxic stressors often result in tumor recurrence. Therefore, a combination therapy with modalities complementary to the vascular-targeting PDT in tumor cell killing or treatments targeting cell surviving and adaptive signaling pathways often shows better results than vascular-targeting PDT alone. These combination regimens should be further evaluated in the clinic. Equally important, we need to further understand the mechanism of vascular-targeting PDT at tissue, cellular, and molecular levels. It is obvious that 100% tumor cure can be achieved in preclinical animal

tumor models with photodynamic vascular targeting therapies. The question is whether it is possible to deliver such curative, rather than subcurative, vascular-targeting PDT to the patients, and how.

Acknowledgment

This work was supported by Department of Defense (DOD) Prostate Cancer Research Grant W81XWH-06-1-0148. The authors would like to gratefully acknowledge QLT Inc. for providing verteporfin.

References

[1] Chen, B., et al., "Vascular and cellular targeting for photodynamic therapy," *Crit Rev Eukaryot Gene Expr*, Vol. 16, 2006, pp. 279–305.

[2] Henderson, B. W., and Dougherty, T. J., "How does photodynamic therapy work?," *Photochem Photobiol*, Vol. 55, 1992, pp. 145–157.

[3] Canti, G., De Simone, A., and Korbelik, M., "Photodynamic therapy and the immune system in experimental oncology," *Photochem Photobiol Sci*, Vol. 1, 2002, pp. 79–80.

[4] Siemann, D. W., Chaplin, D. J., and Horsman, M. R., "Vascular-targeting therapies for treatment of malignant disease," *Cancer*, Vol. 100, 2004, pp. 2491–2499.

[5] Fukumura, D., and Jain, R. K., "Tumor microenvironment abnormalities: causes, consequences, and strategies to normalize," *J Cell Biochem*, Vol. 101, 2007, pp. 937–949.

[6] Siemann, D. W., et al., "Differentiation and definition of vascular-targeted therapies," *Clin Cancer Res*, Vol. 11, 2005, pp. 416–420.

[7] Thorpe, P. E., "Vascular targeting agents as cancer therapeutics," *Clin Cancer Res*, Vol. 10, 2004, pp. 415–427.

[8] Gross, S., et al., "Monitoring photodynamic therapy of solid tumors online by BOLD-contrast MRI," Nat Med, Vol. 9, 2003, pp. 1327–1331.

[9] Fingar, V. H., Wieman, T. J., and Haydon, P. S., "The effects of thrombocytopenia on vessel stasis and macromolecular leakage after photodynamic therapy using photofrin," *Photochem Photobiol*, Vol. 66, 1997, pp. 513–517.

[10] Ben-Hur, E., et al., "Photodynamic treatment of red blood cell concentrates for virus inactivation enhances red blood cell aggregation: protection with antioxidants," *Photochem Photobiol*, Vol. 66, 1997, pp. 509–512.

[11] Fingar, V. H., Wieman, T. J., and Doak, K. W., "Role of thromboxane and prostacyclin release on photodynamic therapy-induced tumor destruction," *Cancer Res*, Vol. 50, 1990, pp. 2599–2603.

[12] Reed, M. W., et al., "The microvascular effects of photodynamic therapy: evidence for a possible role of cyclooxygenase products," *Photochem Photobiol*, Vol. 50, 1989, pp. 419–423.

[13] Foster, T. H., et al., "Photosensitized release of von Willebrand factor from cultured human endothelial cells," *Cancer Res*, Vol. 51, 1991, pp. 3261–3266.

[14] Henderson, B. W., et al., "Effects of photodynamic treatment of platelets or endothelial cells in vitro on platelet aggregation," *Photochem Photobiol*, Vol. 56, 1992, pp. 513–521.

[15] Dolmans, D. E., et al., "Vascular accumulation of a novel photosensitizer, MV6401, causes selective thrombosis in tumor vessels after photodynamic therapy," *Cancer Res*, Vol. 62, 2002, pp. 2151–2156.

[16] Fingar, V. H., "Vascular effects of photodynamic therapy," *J Clin Laser Med Surg*, Vol. 14, 1996, pp. 323–328.

[17] Vaupel, P., and Mayer, A., "Hypoxia in cancer: significance and impact on clinical outcome," *Cancer Metastasis Rev*, Vol. 26, 2007, pp. 225–239.

[18] Fingar, V. H., Wieman, T. J., and Doak, K. W., "Changes in tumor interstitial pressure induced by photodynamic therapy," *Photochem Photobiol*, Vol. 53, 1991, pp. 763–768.

[19] Leunig, M., et al., "Photodynamic therapy-induced alterations in interstitial fluid pressure, volume and water content of an amelanotic melanoma in the hamster," *Br J Cancer*, Vol. 69, 1994, pp. 101-103.

[20] Sporn, L. A., and Foster, T. H., "Photofrin and light induces microtubule depolymerization in cultured human endothelial cells," *Cancer Res*, Vol. 52, 1992, pp. 3443–3448.

[21] Chen, B., et al., "Tumor vascular permeabilization by vascular-targeting photosensitization: effects, mechanism, and therapeutic implications," *Clin Cancer Res*, Vol. 12, 2006, pp. 917–923.

[22] Schmidt-Erfurth, U., et al., "Time course and morphology of vascular effects associated with photodynamic therapy," *Ophthalmology*, Vol. 112, 2005, pp. 2061–2069.

[23] Volanti, C., Matroule, J. Y., and Piette, J., "Involvement of oxidative stress in NF-kappaB activation in endothelial cells treated by photodynamic therapy," *Photochem Photobiol*, Vol. 75, 2002, pp. 36–45.

[24] Volanti, C., et al., "Downregulation of ICAM-1 and VCAM-1 expression in endothelial cells treated by photodynamic therapy," *Oncogene*, Vol. 23, 2004, pp. 8649–8658.

[25] Matroule, J. Y., Volanti, C., and Piette, J., "NF-kappaB in photodynamic therapy: discrepancies of a master regulator," *Photochem Photobiol*, Vol. 82, 2006, pp. 1241–1246.

[26] Korbelik, M., Sun, J., and Cecic, I., "Photodynamic therapy-induced cell surface expression and release of heat shock proteins: relevance for tumor response," *Cancer Res*, Vol. 65, 2005, pp. 1018–1026.

[27] Plaks, V., et al., "Homologous adaptation to oxidative stress induced by the photosensitized Pd-bacteriochlorophyll derivative (WST11) in cultured endothelial cells," *J Biol Chem*, Vol. 279, 2004, pp. 45713–45720.

[28] Chen, B., et al., "Combining vascular and cellular targeting regimens enhances the efficacy of photodynamic therapy," *Int J Radiat Oncol Biol Phys*, Vol. 61, 2005, pp. 1216–1226.

[29] Chen, B., Roskams, T., and de Witte, P. A., "Antivascular tumor eradication by hypericin-mediated photodynamic therapy," *Photochem Photobiol*, Vol. 76, 2002, pp. 509–513.

[30] Boucher, Y., and Jain, R. K., "Microvascular pressure is the principal driving force for interstitial hypertension in solid tumors: implications for vascular collapse," *Cancer Res*, Vol. 52, 1992, pp. 5110–5114.

[31] Rofstad, E. K., et al., "Pulmonary and lymph node metastasis is associated with primary tumor interstitial fluid pressure in human melanoma xenografts," *Cancer Res*, Vol. 62, 2002, pp. 661–664.

[32] Hendrickx, N., et al., "Up-regulation of cyclooxygenase-2 and apoptosis resistance by p38 MAPK in hypericin-mediated photodynamic therapy of human cancer cells," *J Biol Chem*, Vol. 278, 2003, pp. 52231–52239.

[33] Hendrickx, N., et al., "Targeted inhibition of p38alpha MAPK suppresses tumor-associated endothelial cell migration in response to hypericin-based photodynamic therapy," *Biochem Biophys Res Commun*, Vol. 337, 2005, pp. 928–935.

[34] Ferrario, A., et al., "Antiangiogenic treatment enhances photodynamic therapy responsiveness in a mouse mammary carcinoma," *Cancer Res*, Vol. 60, 2000, pp. 4066–4069.

[35] Solban, N., et al., "Mechanistic investigation and implications of photodynamic therapy induction of vascular endothelial growth factor in prostate cancer," *Cancer Res*, Vol. 66, 2006, pp. 5633–5640.

[36] Momma, T., et al., "Photodynamic therapy of orthotopic prostate cancer with benzoporphyrin derivative: local control and distant metastasis," *Cancer Res*, Vol. 58, 1998, pp. 5425–5431.

[37] Pinthus, J. H., et al., "Photodynamic therapy for urological malignancies: past to current approaches," *J Urol*, Vol. 175, 2006, pp. 1201–1207.

[38] Birchler, M., et al., "Selective targeting and photocoagulation of ocular angiogenesis mediated by a phage-derived human antibody fragment," *Nat Biotechnol*, Vol. 17, 1999, pp. 984–988.

[39] Tirand, L., et al., "A peptide competing with VEGF165 binding on neuropilin-1 mediates targeting of a chlorin-type photosensitizer and potentiates its photodynamic activity in human endothelial cells," *J Control Release*, Vol. 111, 2006, pp. 153–164.

[40] Ichikawa, K., et al., "Antiangiogenic photodynamic therapy (PDT) by using long-circulating liposomes modified with peptide specific to angiogenic vessels," *Biochim Biophys Acta*, Vol. 1669, 2005, pp. 69–74.

[41] Reddy, G. R., et al., "Vascular targeted nanoparticles for imaging and treatment of brain tumors," *Clin Cancer Res*, Vol. 12, 2006, pp. 6677–6686.

[42] Frochot, C., et al., "Interest of RGD-containing linear or cyclic peptide targeted tetraphenylchlorin as novel photosensitizers for selective photodynamic activity," *Bioorg Chem*, Vol. 35, 2007, pp. 205–220.

[43] Streckyte, G., et al., "Effects of photodynamic therapy in combination with Adriamycin," *Cancer Lett*, Vol. 146, 1999, pp. 73–86.

[44] Ma, L. W., et al., "Enhanced antitumour effect of photodynamic therapy by microtubule inhibitors," *Cancer Lett,* Vol. 109, 1996, pp. 129–139.

[45] Peng, Q., et al., "Antitumor effect of 5-aminolevulinic acid-mediated photodynamic therapy can be enhanced by the use of a low dose of photofrin in human tumor xenografts," *Cancer Res*, Vol. 61, 2001, pp. 5824–5832.

[46] Dolmans, D. E., et al., "Targeting tumor vasculature and cancer cells in orthotopic breast tumor by fractionated photosensitizer dosing photodynamic therapy," *Cancer Res*, Vol. 62, 2002, pp. 4289–4294.

[47] Jain, R. K., "Delivery of molecular medicine to solid tumors: lessons from in vivo imaging of gene expression and function," *J Control Release*, Vol. 74, 2001, pp. 7–25.

[48] Pogue, B. W., et al., "Analysis of sampling volume and tissue heterogeneity on the in vivo detection of fluorescence," *J Biomed Opt*, Vol. 10, 2005, pp. 41206.

[49] Snyder, J. W., et al., "Photodynamic therapy: a means to enhanced drug delivery to tumors," *Cancer Res*, Vol. 63, 2003, pp. 8126–8131.

[50] Ferrario, A., et al., "Cyclooxygenase-2 inhibitor treatment enhances photodynamic therapy-mediated tumor response," *Cancer Res*, Vol. 62, 2002, pp. 3956–3961.

[51] Ferrario, A., and Gomer, C. J., "Avastin enhances photodynamic therapy treatment of Kaposi's sarcoma in a mouse tumor model," *J Environ Pathol Toxicol Oncol*, Vol. 25, 2006, pp. 251–259.

[52] Kosharskyy, B., et al., "A mechanism-based combination therapy reduces local tumor growth and metastasis in an orthotopic model of prostate cancer," *Cancer Res*, Vol. 66, 2006, pp. 10953–10958.